# Fluid Collections, Cysts and Hematomas

FLUID COLLECTIONS, CYSTS, AND HEMATOMAS

ANTHONY A. MANCUSO

KEY POINTS

- There is great diversity in the appearance of fluid collections on computed tomography, magnetic resonance imaging, and ultrasound.
- Physical properties that interact with imaging parameters producing the diversity of these appearances is important to understand.
- Many cysts that are seen are clinically insignificant.
- Ultrasound is usually not definitive for diagnostic imaging purposes in evaluating cystic neck masses except for thyroid masses.

Tumor, infection, trauma (with or without bleeding and iatrogenic or by other mechanisms), and aberrant development (Chapter 8) can all be associated with cysts, localized fluid collections, and hematomas. Edema confined to a space can mimic a fluid collection.

Cysts, fluid collections, and bleeding occur very commonly in the sinuses. They are also common occurrences in the soft tissues and organ systems of the head and neck. They occur both within bone and beneath the periosteum. There are cysts associated with tumor and regressive cystic changes and bleeding within tumors or tumoral cysts and cystic tumors. Developmental cysts are common in the head and neck, and some, such as venolymphatic vascular malformations (Chapter 9), have bleeding as a complication.

# GENERAL DIAGNOSTIC APPROACH

The general diagnostic approach to the evaluation of cysts, fluid collections, and hematomas or other collections of blood products includes consideration of one or more of the following topics.

## Clinical Setting

The clinical setting virtually always guides the differential diagnosis. The origin and nature of a cyst, hematoma, or other fluid collection is usually not in question after imaging is combined with clinical data. Sampling by aspiration of fluid contents is usually not necessary unless cancer or infection is suspected. A partial list of some examples of common associated clinical circumstances follows:

- A history or acute setting of trauma raises the possibility of hematoma or posttraumatic hematocyst (Fig. 10.1).

**FIGURE 10.1.** Non–contrast-enhanced computed tomography showing the density of the acute hematoma contributing to the airway obstruction in this trauma patient to be greater than that of muscle.

- A rapid increase in size suggests bleeding or bleeding into a pre-existing lesion. (Fig. 10.2)

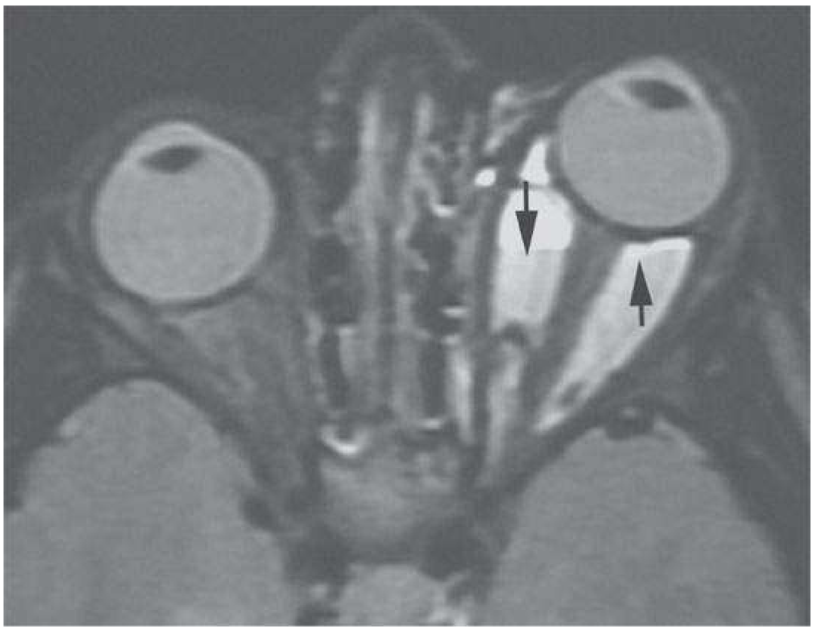

**FIGURE 10.2.** Short T1 inversion recovery (STIR) magnetic resonance image of a patient who presented with acute enlargement of an orbital mass. Fluid–fluid levels *(arrows)* are likely related to blood products.

- A history of fluctuating size suggests a developmental lesion that may be liable to intermittent inflammation, one that may contain tissue responsive to inflammation, or one that communicates with the outside world somehow by a tract or fistula (Fig. 10.3).[1,2]

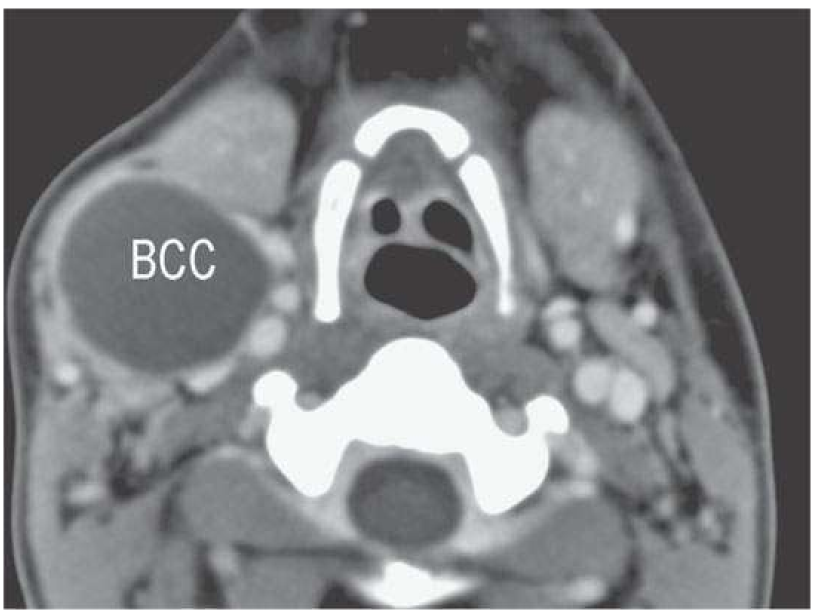


**FIGURE 10.3.** Contrast-enhanced computed tomography of a second branchial cleft cyst *(BCC)* with a smooth thin wall and no surrounding inflammatory changes.

- Steady progressive enlargement over a protracted period of time without pain or signs of inflammation suggests a neoplasm (Fig. 10.4).[1–3]

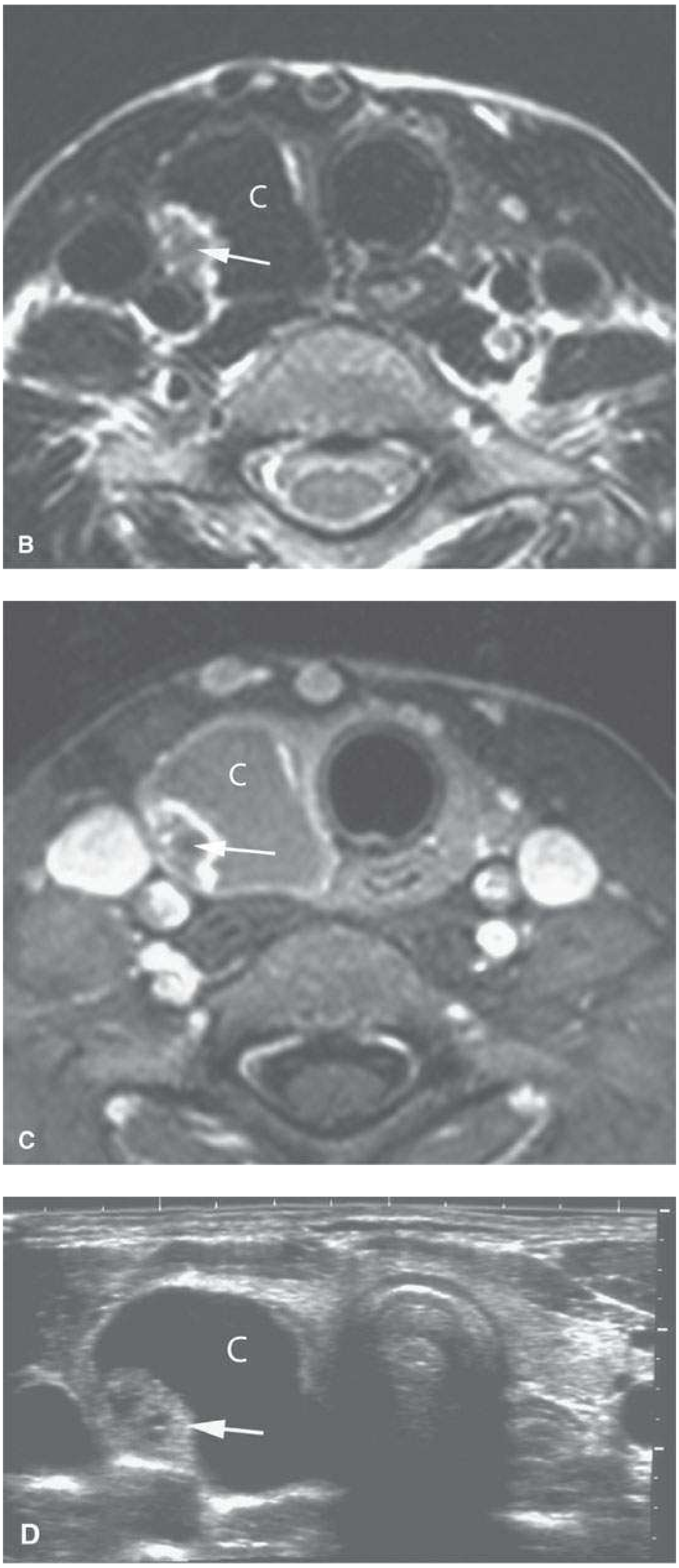
C
B
C
C
C
D

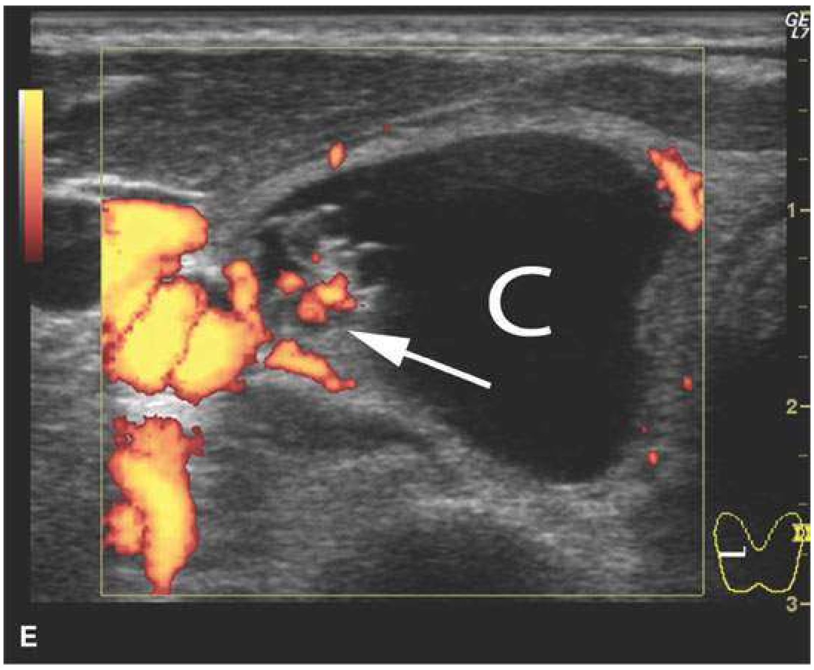


**FIGURE 10.4.** Patient with an enlarging low neck mass imaged first with ultrasound and then magnetic resonance imaging showing a cyst **(C)** and associated nodule in all of the following images. **A:** T1-weighted non–contrast-enhanced image showing a high signal intensity cyst suggesting that it contains colloid or blood products associated with a nodule *(arrow)*. **B:** T2- weighted image shows the cyst to be of very low signal intensity suggesting the presence of blood products or desiccated colloid, but fibrosis or calcification would not seem to be reasonable alternative explanations based on all of the imaging findings. **C:** T1-weighted fat-suppressed contrast-enhanced magnetic resonance image shows that the cyst wall does not enhance and that the nodule is irregular and obviously vascularized. **D:** Comparison transverse B-mode ultrasound. **E:** Color flow ultrasound image shows that the nodule is not only irregular but also well vascularized.

- Fever, poor feeding, and pharyngitis with retropharyngeal edema in a young child suggest a suppurative retropharyngeal lymph node (Fig. 10.5).

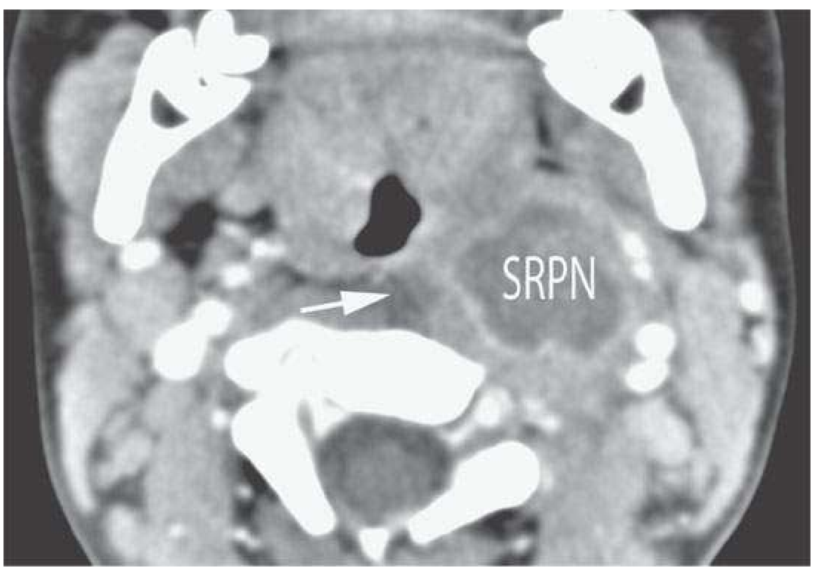


**FIGURE 10.5.** Contrast-enhanced computed tomography in a 1-year-old child with partially treated suppurative retropharyngeal adenitis. The suppurative node *(SRN)* has a minimally enhancing margin and relatively low grade surrounding inflammatory response and a small amount of retropharyngeal edema *(arrow)*.

## Normal Variant and Common, or Incidental and Unimportant

Cysts or fluid collections are often anatomic variations such as the Tornwaldt cyst of the nasopharynx (Fig. 10.6).4 Cysts or fluid collections may also be totally innocuous, such as the very common postinflammatory cysts in the Waldeyer ring lymphoid tissue (Fig. 10.7) or simple mucous or retention cysts in the sinuses.1–3 Such variants should be recognized as unimportant clinically, but they do allow a study of the appearance of cyst contents in a way that might prove helpful in understanding cysts and fluid collections that do have some consequence.

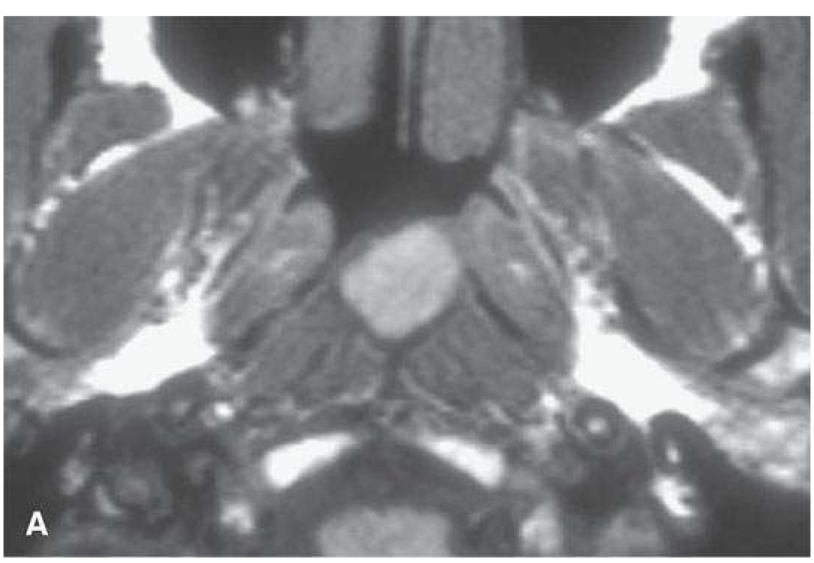


**FIGURE 10.6.** Magnetic resonance imaging of an incidental Tornwaldt's cyst. **A:** T1-weighted image shows high signal intensity almost approaching that of fat. **B:** T2-weighted image shows the cyst contents to be much less intense than cerebrospinal fluid, likely related to the mucoid nature of those cyst contents.

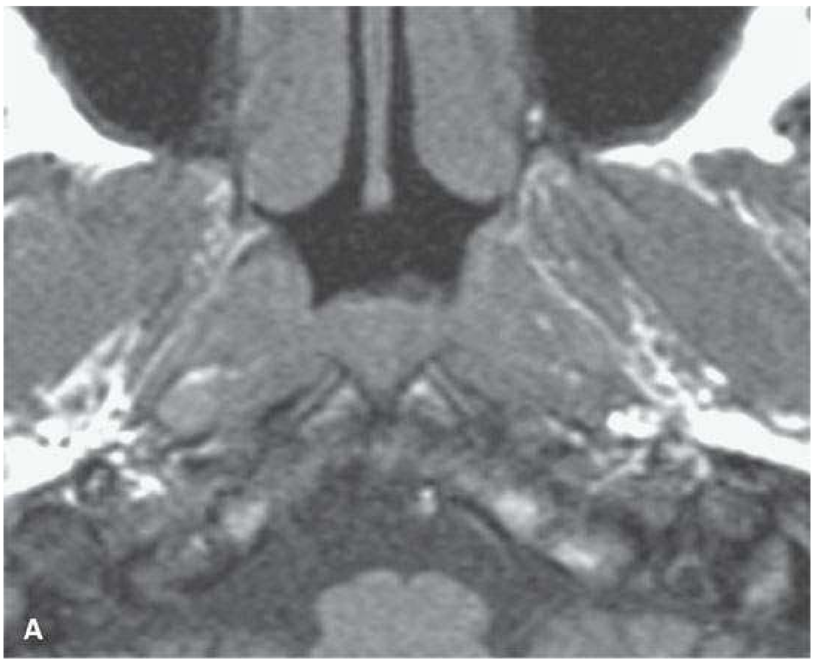


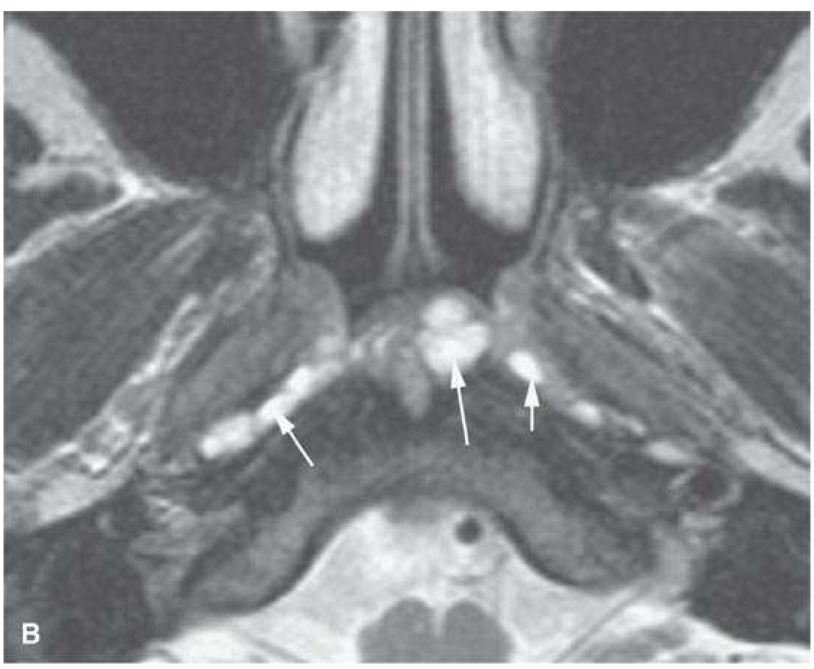

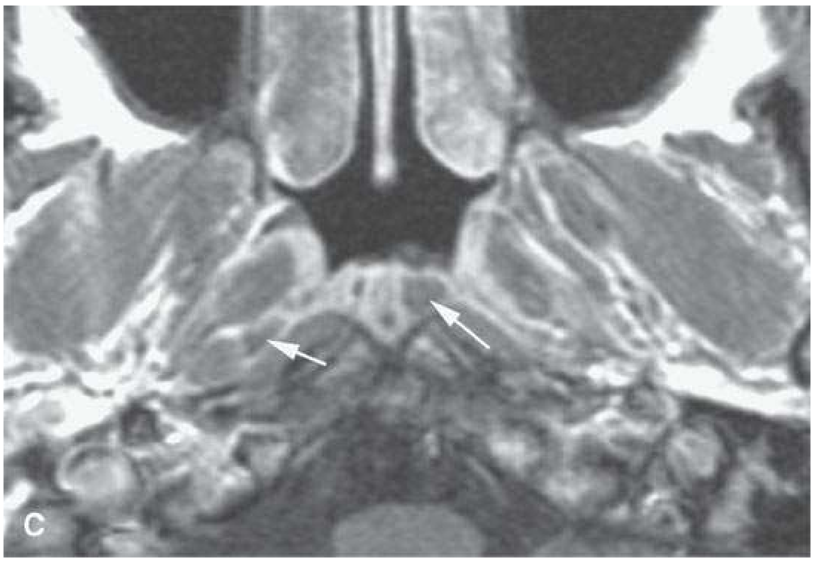


**FIGURE 10.7.** Magnetic resonance imaging of incidental and clinically insignificant retention or postinflammatory cysts in the adenoids. **A:** On T1-weighted images, the cysts are isointense to the normal lymphoid tissue. **B:** On T2-weighted images, the cysts become far more conspicuous *(arrows)*. **C:** Contrast-enhanced T1-weighted images shows the cysts differentiated from the normally enhancing lymphoid tissue *(arrows)*.

## Solitary or Multiple Cysts

If cysts or cystic masses are multiple, and especially if they are multiple and bilateral, they can suggest systemic diseases as diverse as basal cell nevus syndrome and HIV infection, depending on their anatomic distribution (Fig. 10.8). One the other hand, unilateral multiple parotid and periparotid cystic masses suggest a Warthin tumor or metastatic skin cancer to regional parotid nodes.


**FIGURE 10.8.** Contrast-enhanced computed tomography of an HIV patient with bilateral lymphoepithelial cysts.

Multiple cystic lesions in the neck raise the possibility of lymphadenopathy.1–3 The pattern of disease and clinical situation usually clarify the likely etiology to no more than two choices (Fig. 10.9).

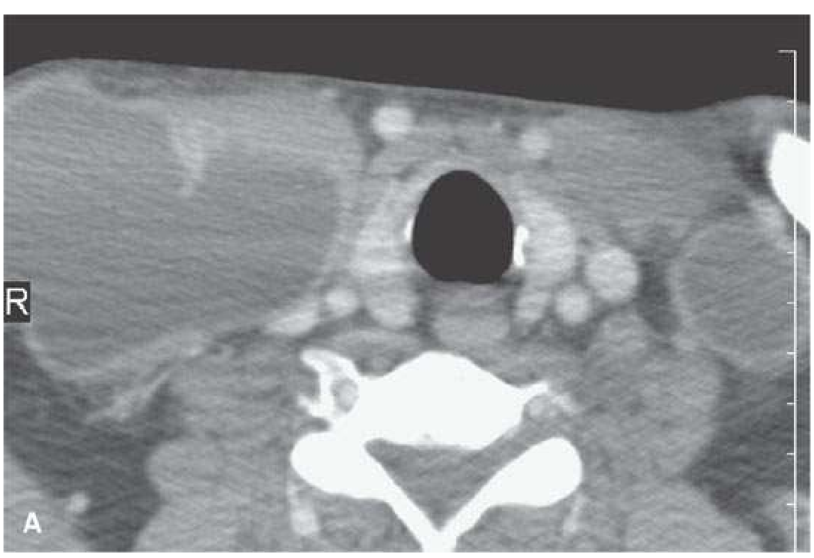

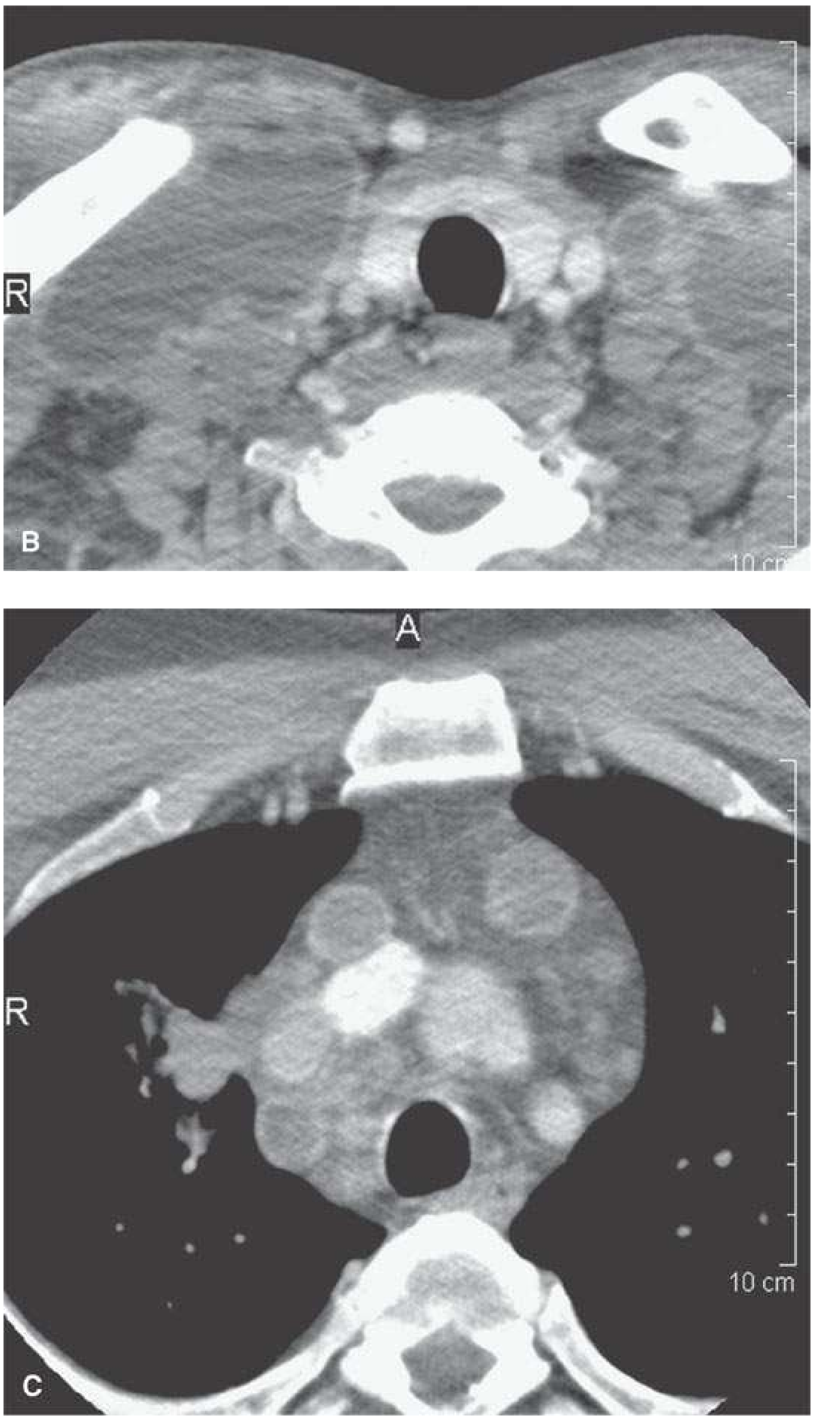


FIGURE 10.9. Contrast-enhanced computed tomography of an HIV-positive patient with bilateral neck masses. **A–C:** Multiple, bilateral cystic masses and obviously mediastinal adenopathy. The walls of the nodes enhance minimally, and there is a relatively low grade inflammatory response surrounding the nodes in both the neck and the mediastinum.

## Anatomic Relationships

Decisions about whether a predominantly cystic mass is a nodal versus nonnodal etiology is largely driven by anatomy.

Developmental cysts such as those of the branchial apparatus (Figs. 10.10, 10.11 and 10.12) and thyroglossal duct (Figs. 10.13 and 10.14) often bear a characteristic relationship to the pharynx and other neck viscera, but some ambiguity in a purely anatomic differentiation arises in differentiation of second branchial cleft cysts and necrotic or otherwise cystic level 2A lymph nodes (Fig. 10.11).5–7

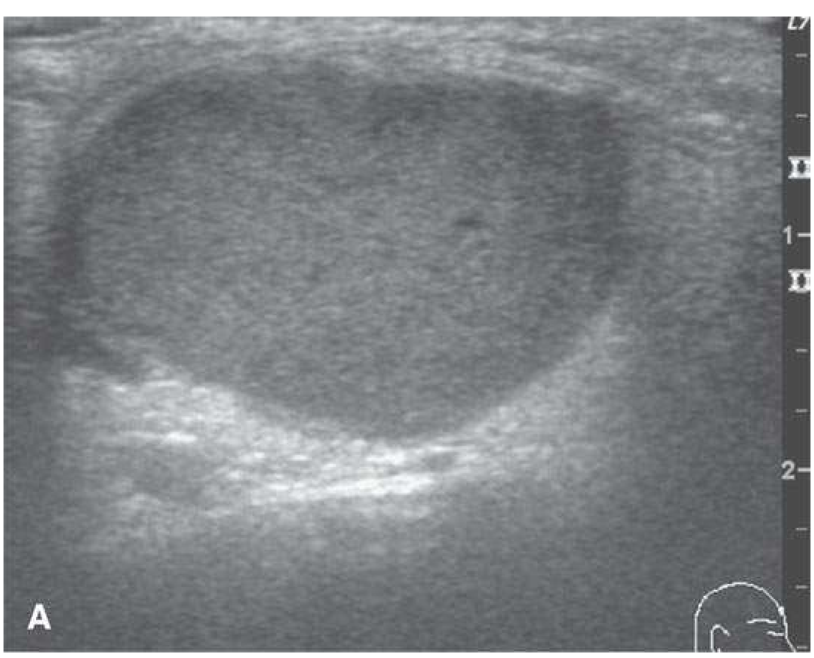


**FIGURE 10.10.** Ultrasound of a right-sided neck mass subsequently proven to be a second branchial cleft cyst. The color flow images showed displaced vessels and confirmed that the mass itself was not vascular. The ultrasound was only marginally useful in the diagnostic process for these purposes.


**FIGURE 10.11.** Contrast-enhanced computed tomography of a second branchial cleft cyst with a thick nodular wall *(arrows)* and relatively low grade inflammatory changes in the surrounding fat *(arrowheads)*.

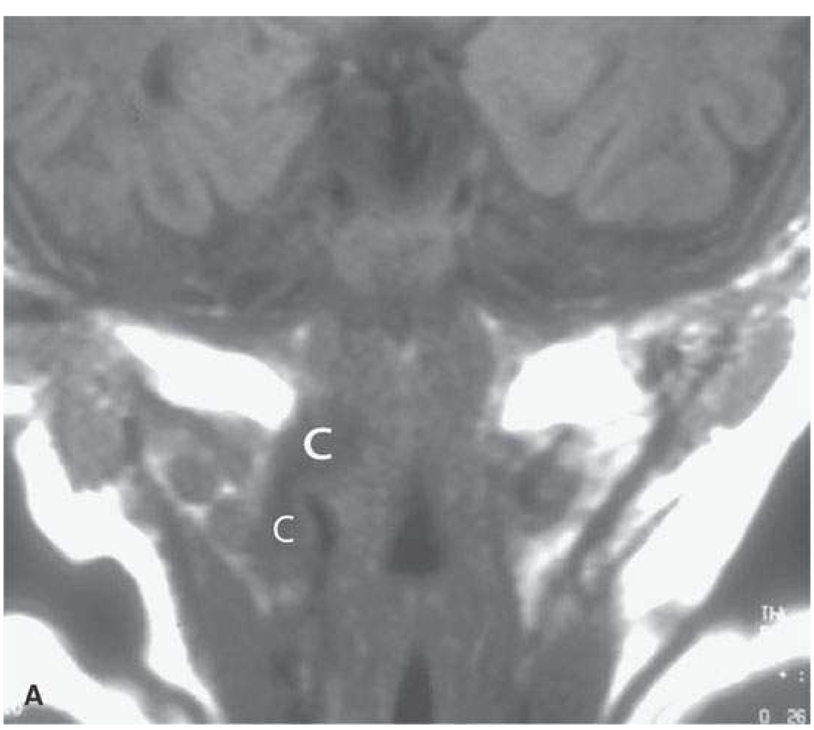

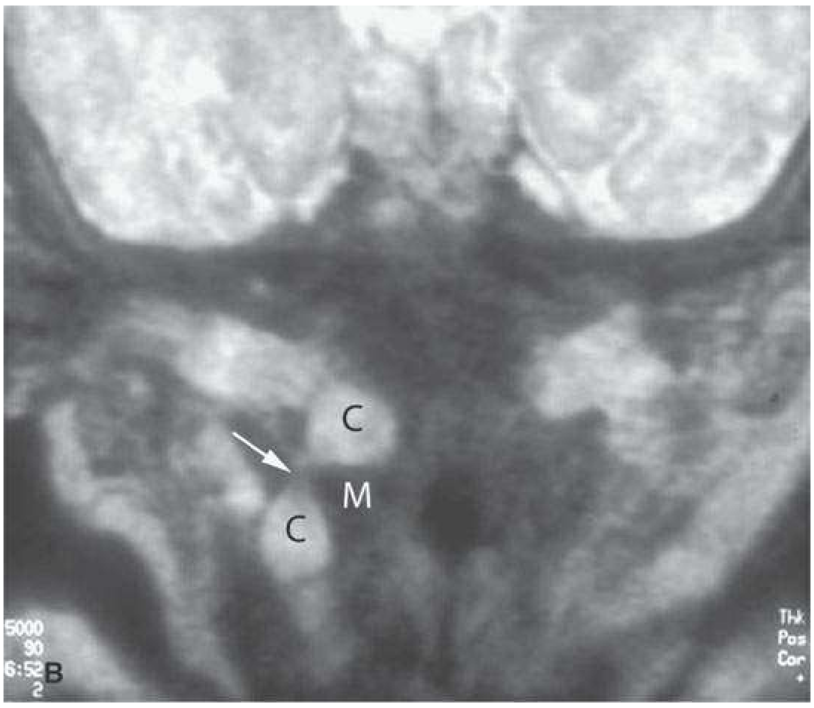


**FIGURE 10.12.** Magnetic resonance imaging of an infant with a pharyngeal wall mass. In both the T-weighted **(A)** and T2-weighted **(B)** images, the cystic structure **(C)** can be seen. Its appearance as it crosses the muscular **(M)** pharyngeal wall *(arrow)* to extend from the pharynx into the neck is an anatomic pattern unmistakably recognizable as a branchial apparatus anomaly, even though this particular type of cyst is rare.

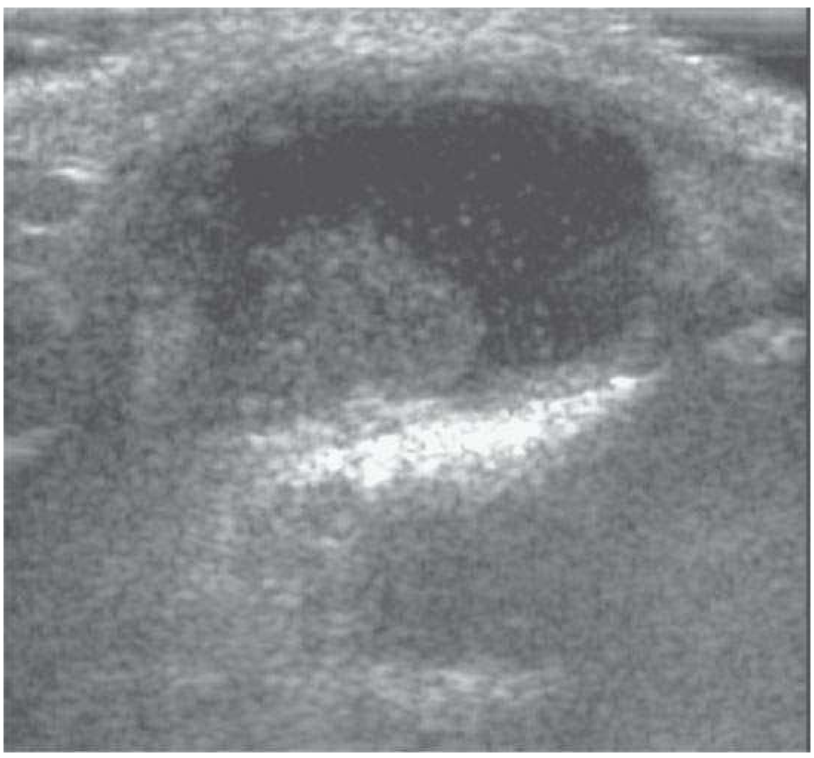

**FIGURE 10.13.** Ultrasound of a pediatric patient believed to have a thyroglossal duct cyst. The study showed a cyst and a nodule but was not anatomically complete enough to confirm the diagnosis of a thyroglossal duct cyst. In essence, these were resources and time that might have been better spent.

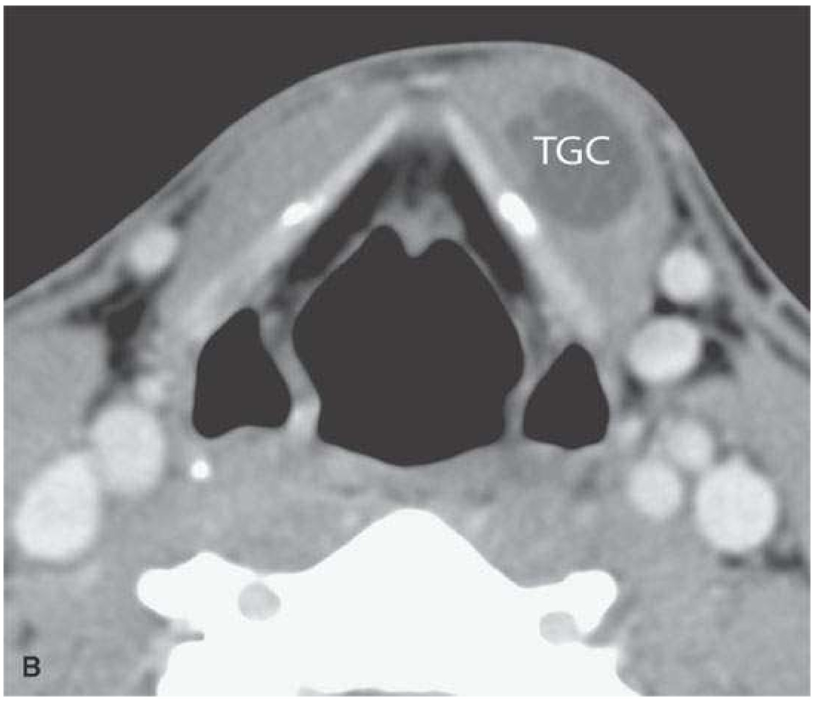


**FIGURE 10.14.** Contrast-enhanced computed tomography of a patient suspect of having a thyroglossal duct cyst. The study, two images from which are seen in **(A)** and **(B)**, confirmed the diagnosis and the full extent of the thyroglossal duct cyst *(TGC)*, allowing for proper surgical planning of a modified Sistrunk procedure.

The sinonasal region, salivary glands, thyroid gland, and all other viscera have a tendency to be associated with certain types of cysts, fluid collections, and patterns of bleeding. For instance, serous and mucous retention cysts will be submucosal within the sinus cavity, and HIV-related epithelial cysts will be partially solid and usually bilateral in the parotid and sometimes submandibular glands (Fig. 10.8). Colloid cysts and cystic adenomas of the thyroid gland are ubiquitous, and some predominantly cystic masses may be thyroid cancer (Fig. 10.15).

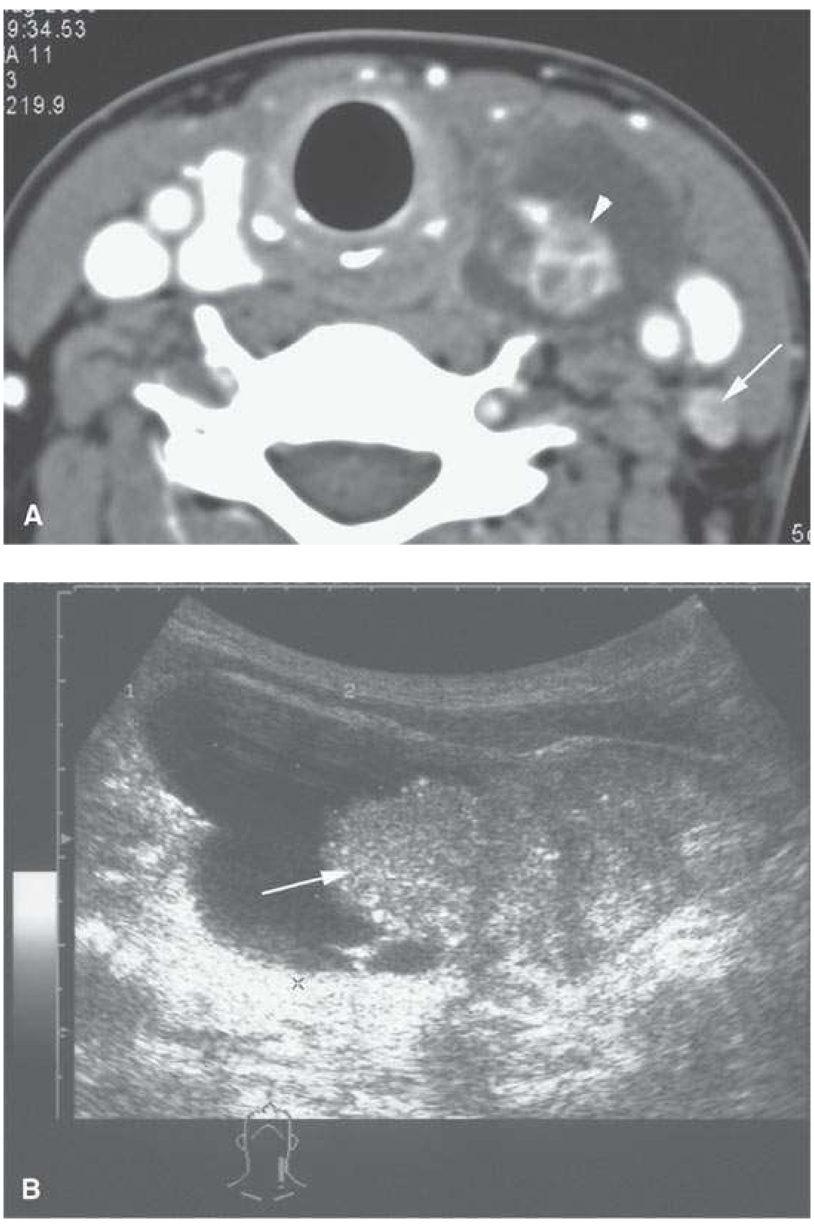

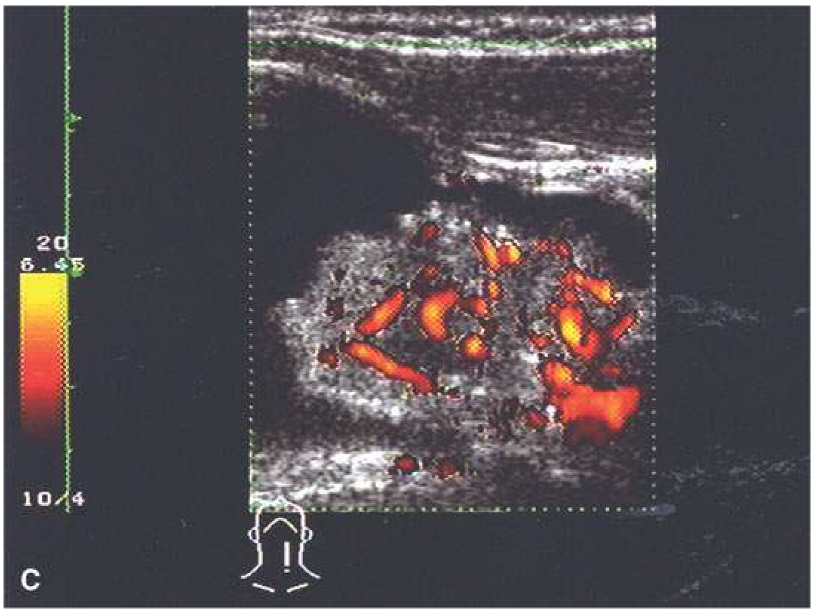


**FIGURE 10.15.** Patient with an enlarging low neck mass imaged first with ultrasound and then contrast-enhanced computed tomography (CECT) showing a cyst and associated nodule in all of the following images. **A:** CECT image showing an irregular nodule with a cyst that shows calcification, possibly psammomatous, and an enhancing metastatic level 4 lymph node *(arrow)*. **B:** Ultrasound showing an irregular nodule and some shadowing suggestive of psammomatous calcification. **E:** Color flow image shows that the nodule is not only irregular but also well vascularized.

Edema confined to a known anatomic space such as the retropharyngeal space may mimic a fluid collection.

Postoperative fluid collections in the low neck and supraclavicular fossa may be related to injury to the thoracic duct or other major lymphatic collecting trunks in this region (Fig. 10.16). Postoperative seromas typically accumulate in the anterior and/or posterior triangles and deep to the closure of the superficial fascia or deeper fascial layers of the neck after a surgical procedure, the most common being a neck dissection (Figs. 10.17–10.20).


**FIGURE 10.16.** Contrast-enhanced computed tomography of the normal thoracic duct. **A:** Fluid density structure with no visible wall *(arrow)* is another example of a consistently visible normal cystic structure that is visible on modern imaging studies. **B:** Oblique reformations show the thoracic duct *(arrow)* near its connection to the subclavian vein.


**FIGURE 10.17.** Contrast-enhanced computed tomography show a small seroma **(S)** in the posterior triangle with no enhancement at its margins.

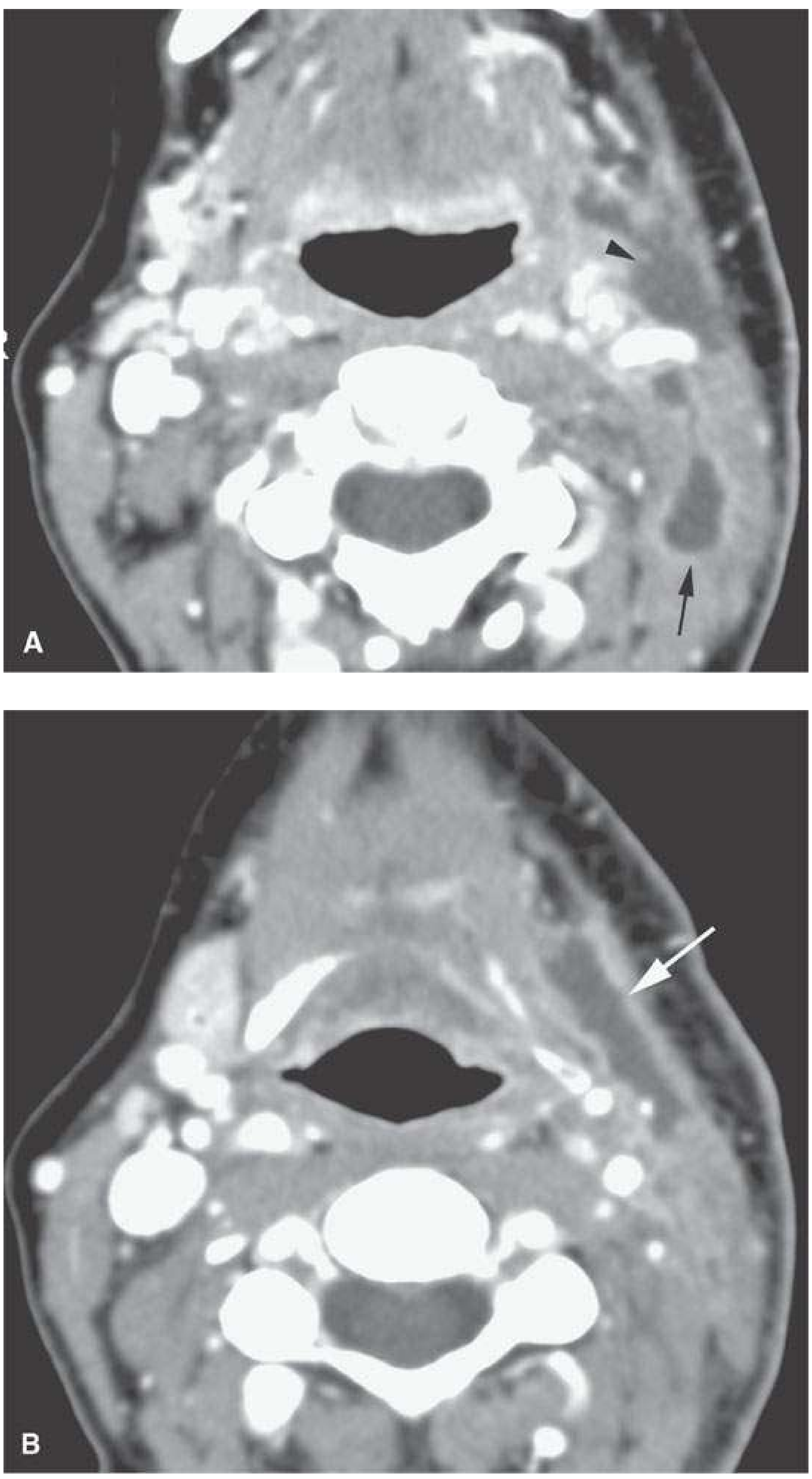

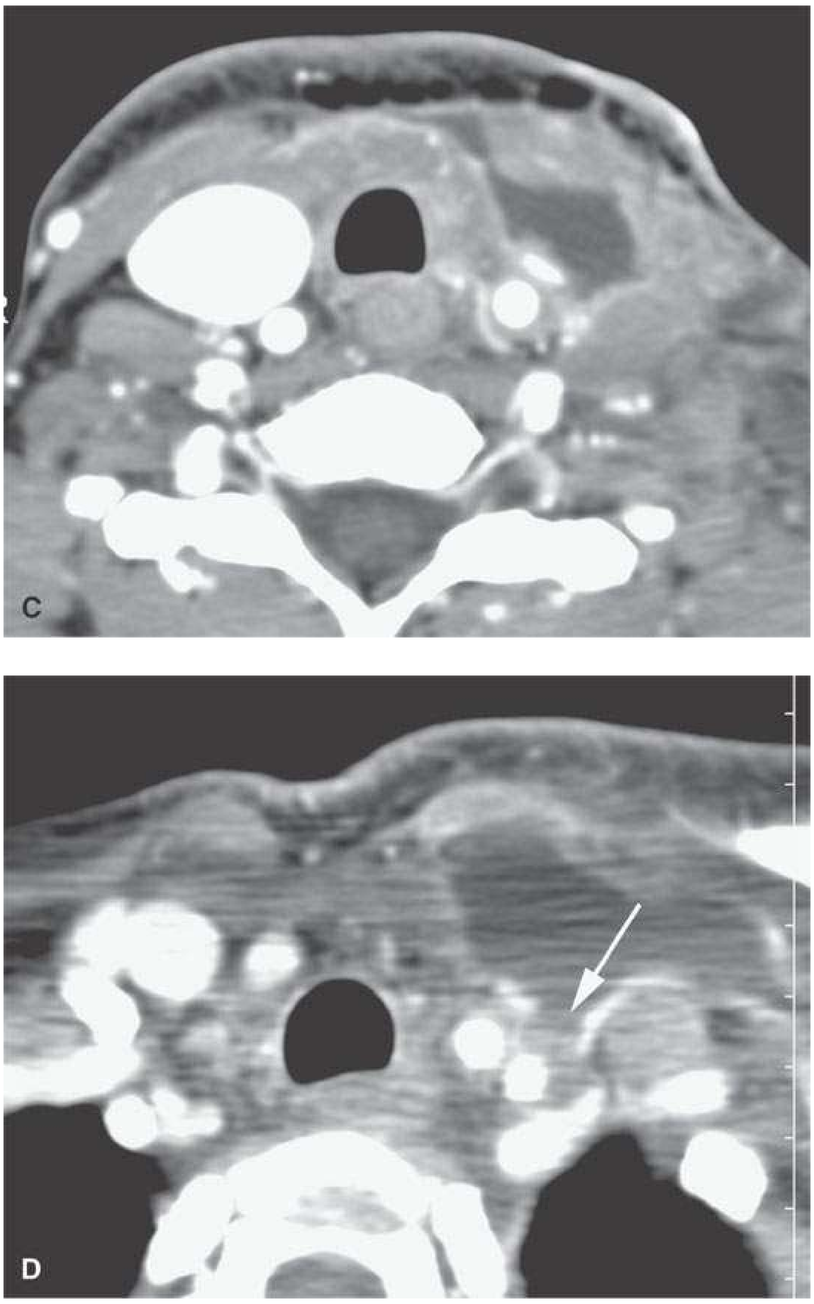


**FIGURE 10.18.** Contrast-enhanced computed tomography showing a postoperative seroma and chyle leak. Some areas of the fluid collection show reactive enhancement along its margins (*arrow* in **A**) while others do not (*arrowhead* in **A**). **A, B:** The collection lies deep to the closure of the superficial fascia *(arrows)* and around the carotid sheath and in the posterior triangle. **C, D:** The collection is mainly deep to the investing layer of cervical fascia and then projects into the region where the thoracic duct joins the subclavian vein *(arrow)* suggestive of a chyle leak, explaining at least part of the fluid collection.

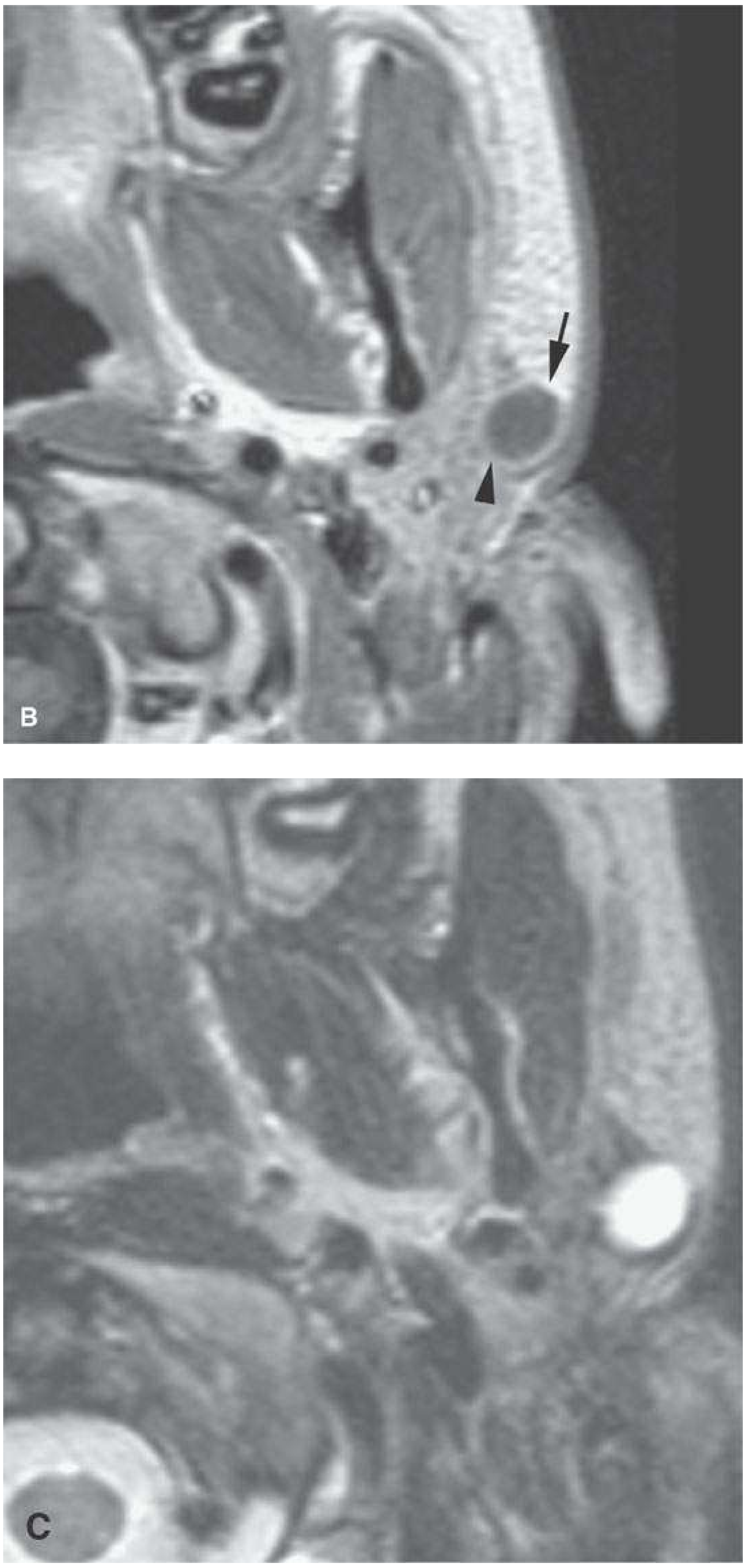


**FIGURE 10.19.** Magnetic resonance imaging of a small postoperative seroma in the parotid gland. **A**: T1-weighted non–contrast-enhanced image showing the seroma **(S)** to be isointense to the parotid and muscle. **B**: T1-weighted contrast-enhanced image improves the contrast between the enhancing remaining parotid tissue and the seroma, but the enhancing margin that is seen well in contrast to the glandular tissue *(arrowhead)* is lost in comparison to fat *(arrow)*. **C**: T2-weighted image, with the seroma to be obviously fluid.

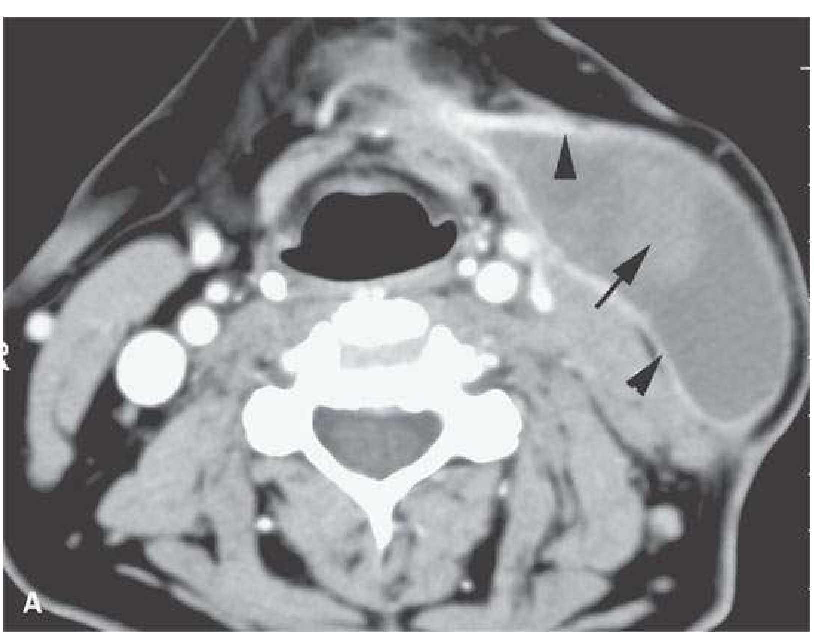

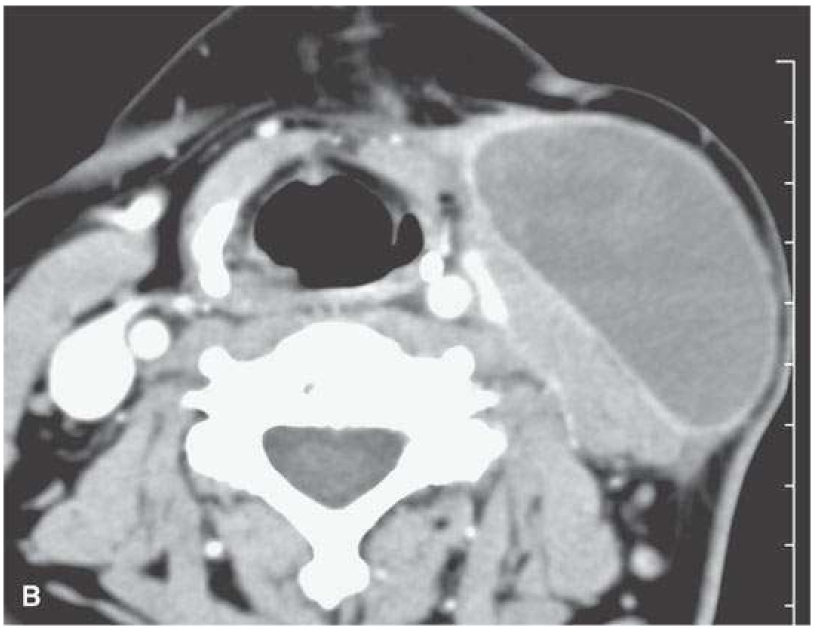


**FIGURE 10.20.** Contrast-enhanced computed tomography of a postoperative hematoma evolving to a seroma. **A:** Organized clot is still visible *(arrow)* within the fluid collection that has a minimally enhancing reactive pseudocapsule *(arrowheads)*. **B:** A section lower in the neck shows only the fluid as it collects between the superficial and the investing layer of deep cervical fascia. The enhancing pseudocapsule is likely composed in part by these fascial layers *(black arrows)*, reflecting that the hematoma occurred deep to the closure of the superficial fascia since it is separate from the subcutaneous fat *(white arrows)*.

## Distribution and Growth Patterns

Postoperative fluid collections will tend to conform to the operative space and are also shaped by the method of closing that space (Figs. 10.18 and 10.20).

Dermoid and epidermoid cysts have particular intracranial and extracranial sites of predilection related to embryologic development (Chapter 8) and may enter into the differential diagnosis of a fluid collection when the clinical situation does not make this differentiation clear (Fig. 10.21).

**FIGURE 10.21.** Contrast-enhanced computed tomography of what was believed to be an atypical dermoid or epidermoid cyst but what proved to be mucous retention cysts at surgery. The atypical nature of there being two separate cysts might have been a clue to this unusual diagnosis.

## Morphologic Features

Infected collections are described in detail in conjunction with the general discussion the morphology and imaging characteristics of abscesses and other infections (Figs. 10.21 and 10.22 and Chapter 13). This discussion deals primarily with noninfected fluid collections ranging from developmental cysts to postoperative seromas or chyle leaks.

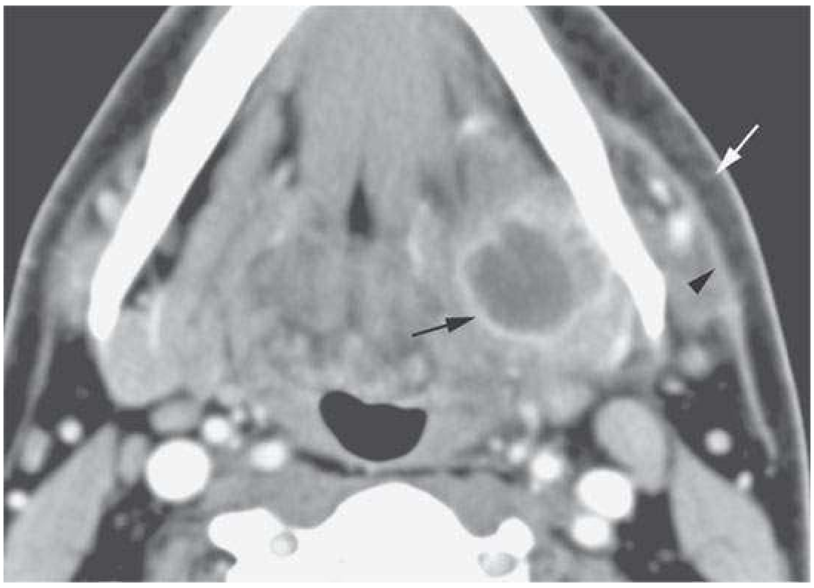

**FIGURE 10.22.** Contrast-enhanced computed tomography of a patient with an acute, untreated abscess of the floor of the mouth and submandibular space with typical features including a thick enhancing rim *(black arrow)*, low-density contents, and surrounding cellulitis and edema manifest by thickening of the superficial musculoaponeurotic system (SMAS) layer *(arrowhead)* and subcutaneous edema *(white arrow)*.

Useful morphologic features to note in forming opinions about the origin and etiology of a “cyst” or fluid collection include location; presence of an associated mass (Figs. 10.4 and 10.15); presence and enhancement of a capsule or pseudocapsule; nodularity or focal enhancement of the “containing wall” (Fig. 10.11); calcification (Fig. 10.24); and surrounding reactive change (Fig. 10.22), septations (Fig. 10.25), fluid–fluid levels (Figs. 10.2 and 10.25), fat, gas, and the “consistency” of the fluid (Figs. 10.6 and 10.26). The nature of the fluid or other contents can be evaluated more comprehensively with magnetic resonance imaging (MRI) than computed tomography (CT) based on relaxation properties as estimated from standard T1-weighted (T1W) and T2-weighted (T2W) images and data available from diffusion-weighted imaging (DWI) (Figs. 10.27–10.29). Fatty content, cholesterol or otherwise, (Fig. 10.30) suggests a developmental cyst (Chapter 8). The nature of the consistency of fluid is discussed more fully subsequently.

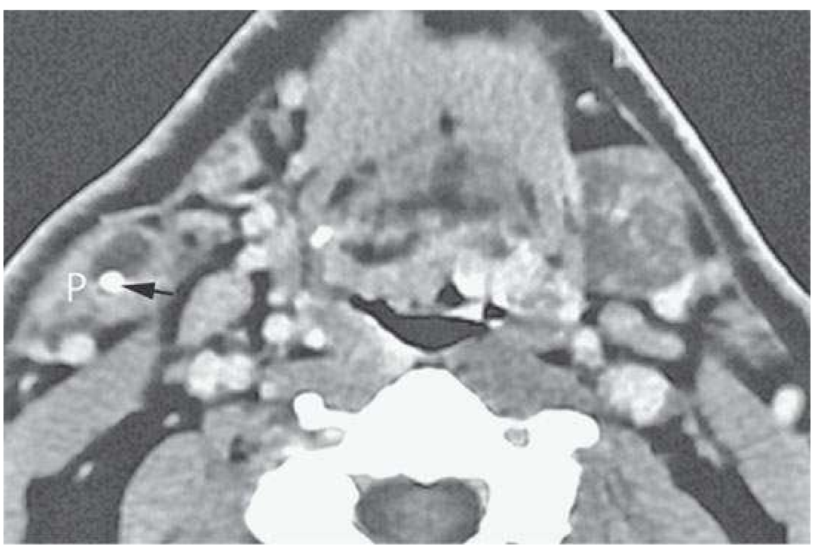


**FIGURE 10.24.** Contrast-enhanced computed tomography of a patent with a parotid tail **(P)** mass that is actually a small sialocele, with the associated calcification *(arrow)* perhaps an indicator of the likely inflammatory nature of the parotid “mass.”

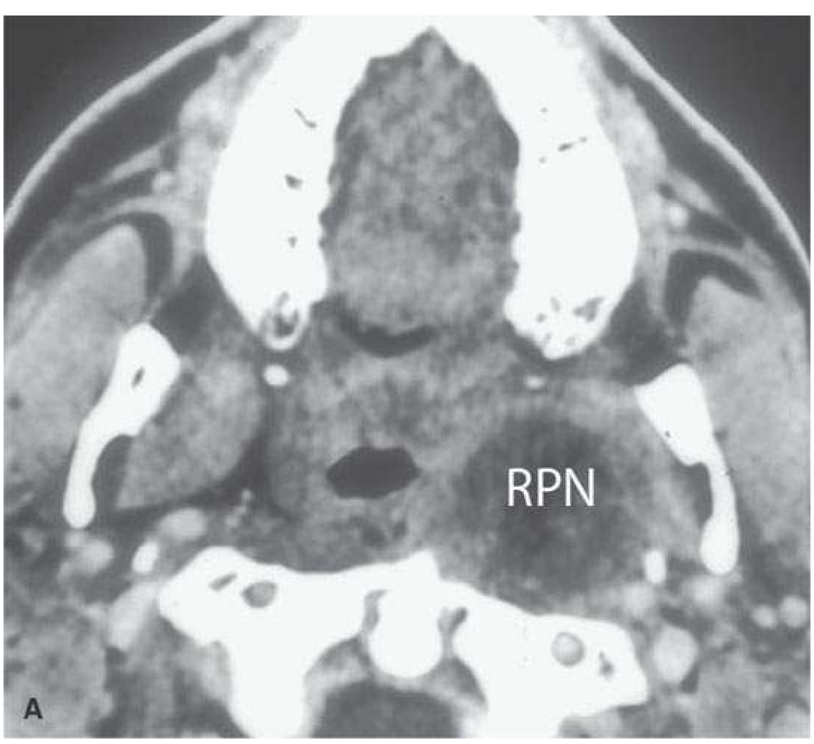

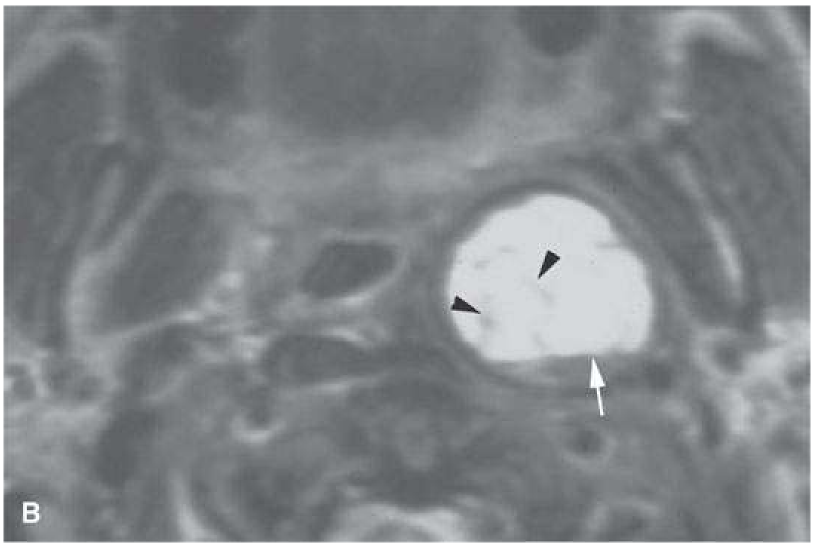


**FIGURE 10.25.** Contrast-enhanced computed tomography (CT) **(A)** and T2-weighted magnetic resonance imaging (MRI) **(B)** of a thick-walled but predominantly low-density (on CT) metastatic retropharyngeal lymph node *(RPN)* in a patient treated for nasopharyngeal cancer. The MRI shows a fluid–fluid level *(arrow)* and septae *(arrowheads)* illustrating the lack of specificity of such imaging findings.


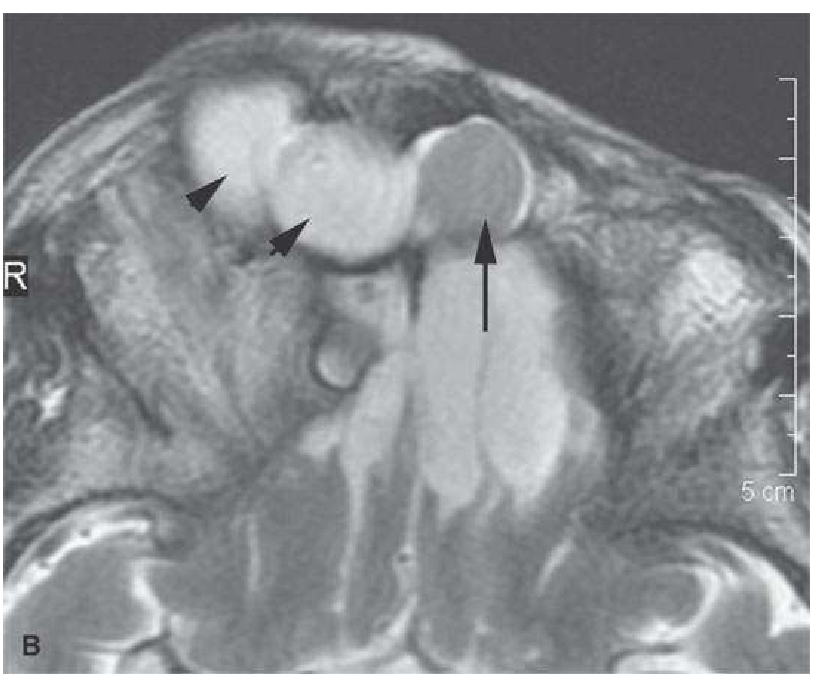

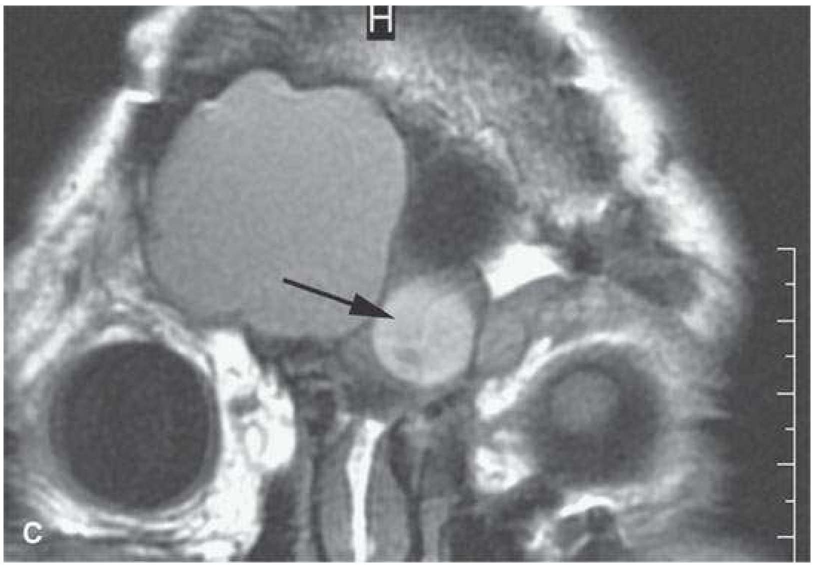


**FIGURE 10.26.** Computed tomography (CT) and magnetic resonance (MR) imaging of a patient with posttraumatic mucoceles. **A:** CT shows densities about equivalent to water *(arrowheads)*, and progressively becoming more dense (*white arrow* and *black arrow*). **B:** T2-weighted MR image shows differing signal intensities (*arrowheads* and *arrows*). **C:** T1-weighted images show varying signal intensities in the multiple components of this complex mucocele, with the brightest one on this image correlating with the one with the least signal intensity in (B).

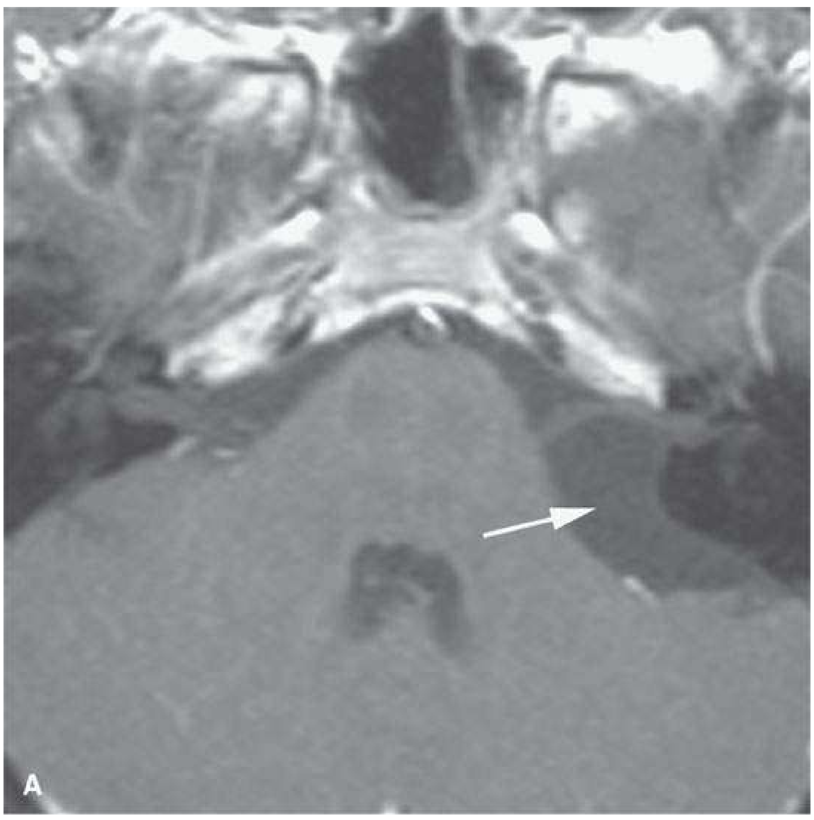


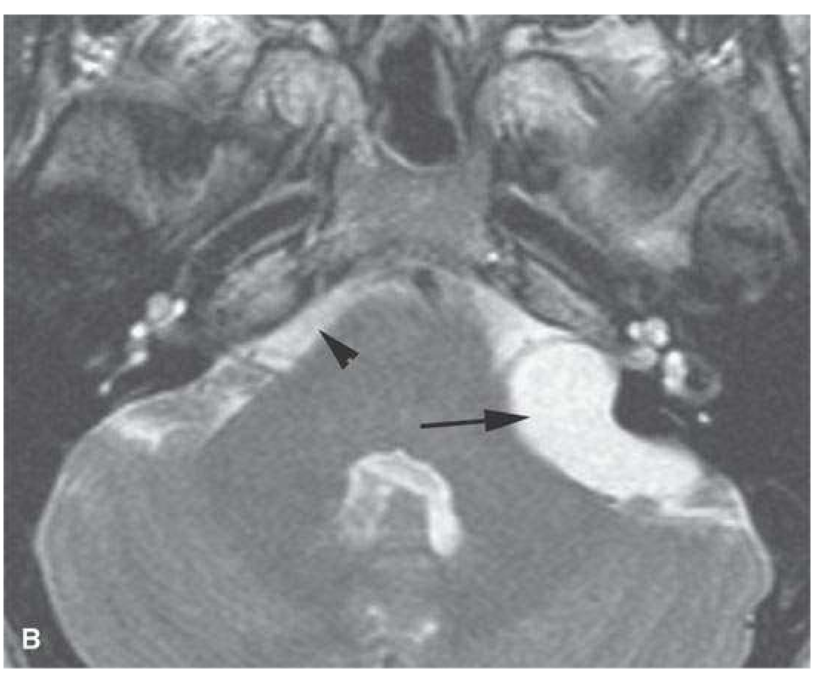

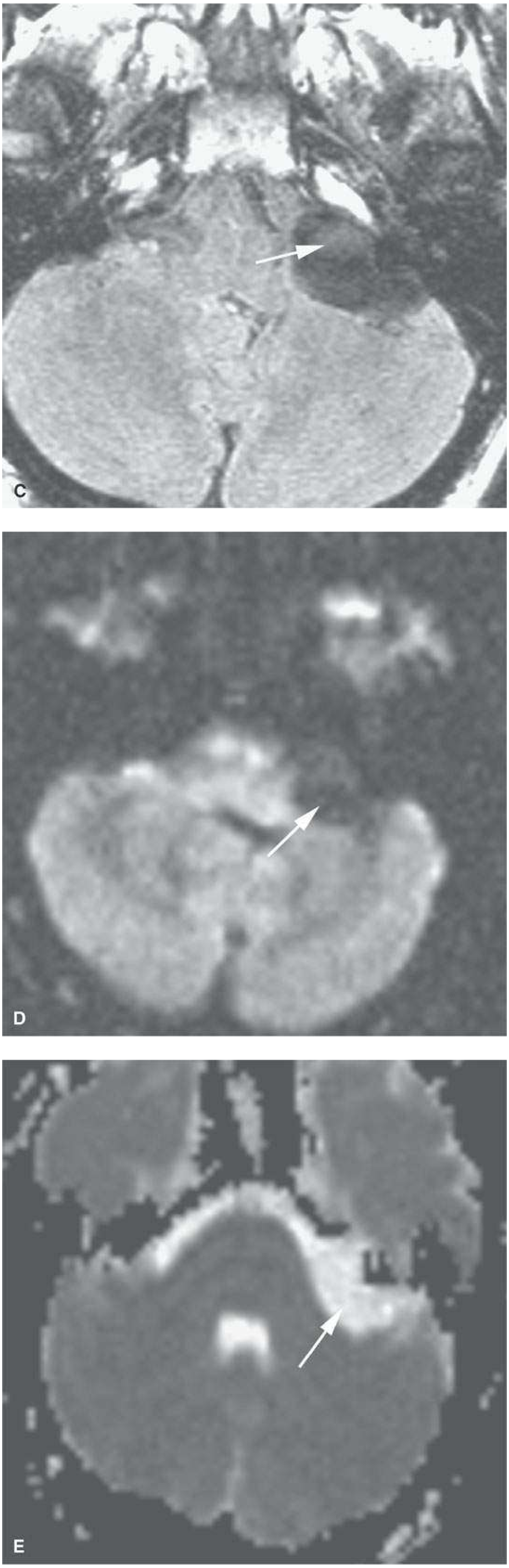
C
D
E

**FIGURE 10.27.** Magnetic resonance imaging of a patient with a cerebellopontine angle (CPA) arachnoid cyst. **A:** T1-weighted images shows the cyst *(arrow)* displacing the nerves and remodeling of the petrous bone. **B:** T2-weighted image shows the same findings as in **(A)** and that the relatively static fluid in the cyst is brighter than the cerebrospinal fluid (CSF) in the contralateral CPA *(arrowhead)*. **C:** Fluid attenuation inversion recovery (FLAIR) image is relatively motion sensitive, and the brighter signal in the cyst *(arrow)* is due to CSF motion. **D, E:** These images show no evidence of restricted diffusion in the cyst *(arrows)*.

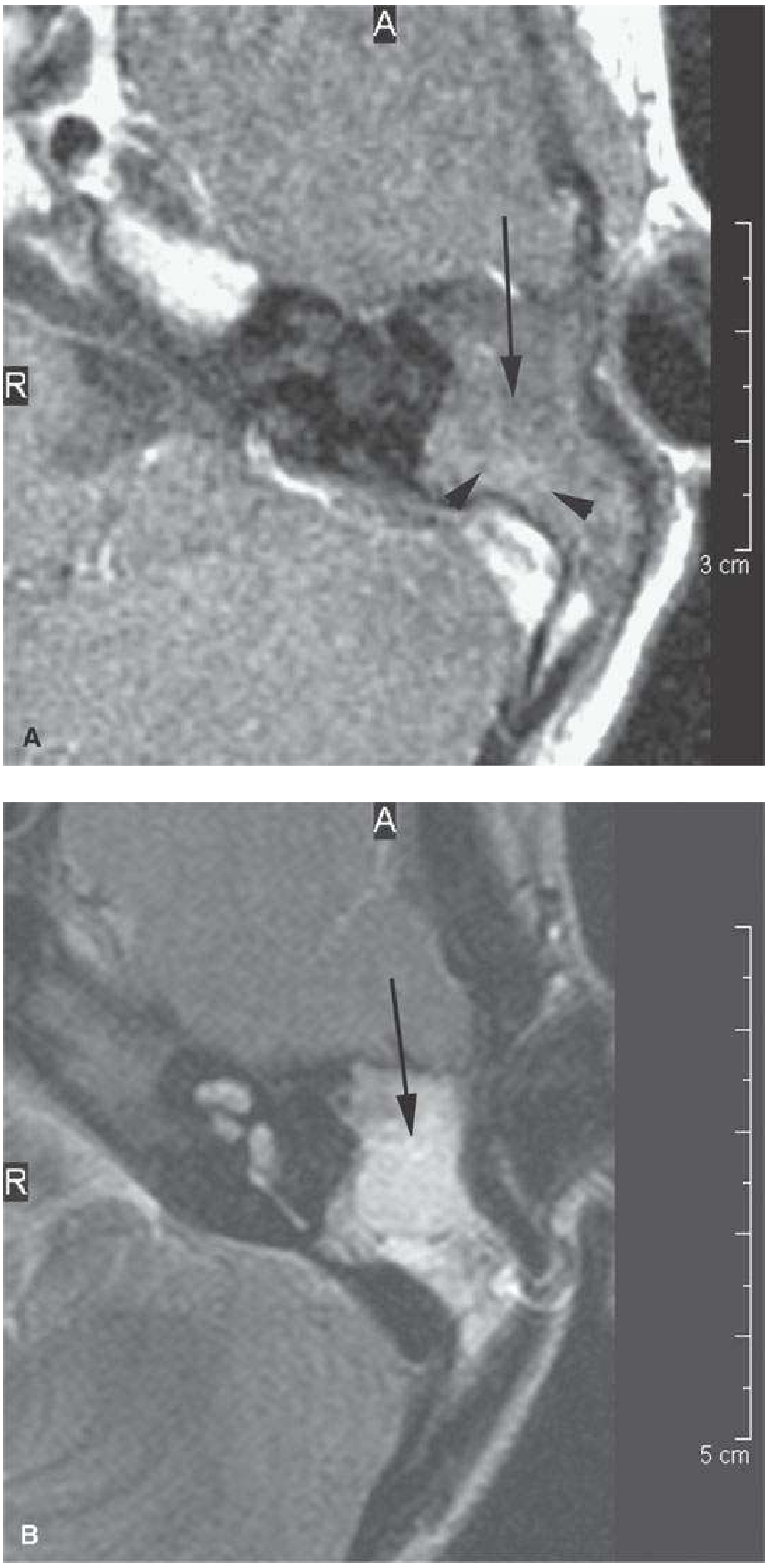

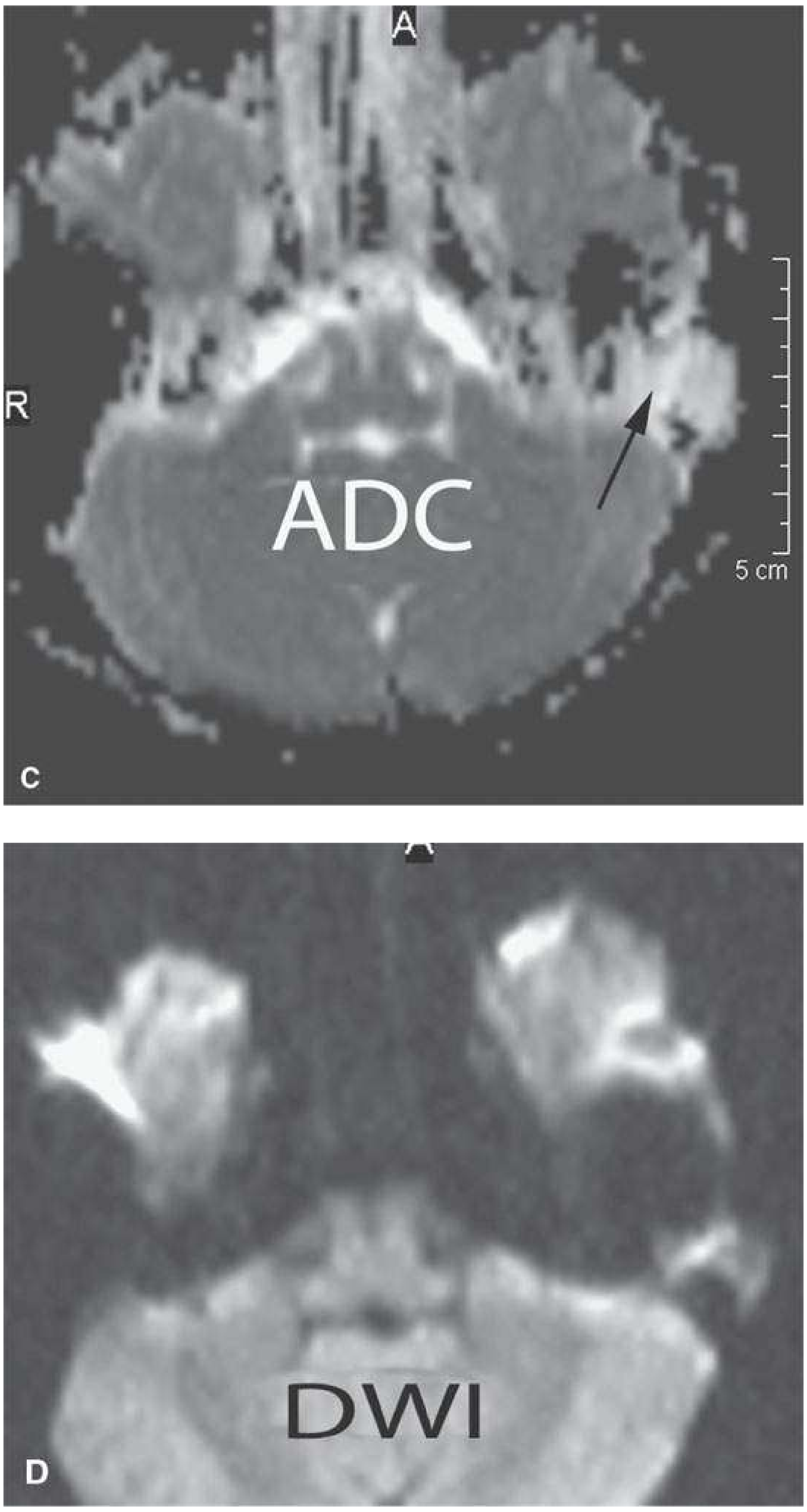


**FIGURE 10.28.** Patient with draining mastoid and ambiguous computed tomography findings with regard to whether there was recurrent cholesteatoma. **A:** T1-weighted image shows areas that are isointense to brain *(arrow)* and some slightly more intense *(arrowheads)* in this heterogeneous collection that is not obviously fluid based on this image. **B:** T2-weighted image shows a relatively homogenous cerebrospinal fluid equivalent signal that does not distinguish fluid from recurrent cholesteatoma. **C:** Diffusion-weighted image shows possibly restricted diffusion, which is not confirmed in the apparent diffusion coefficient (ADC) map **(D)** *(arrow)*. Preoperative diagnosis was no cholesteatoma, and this was confirmed at surgery.

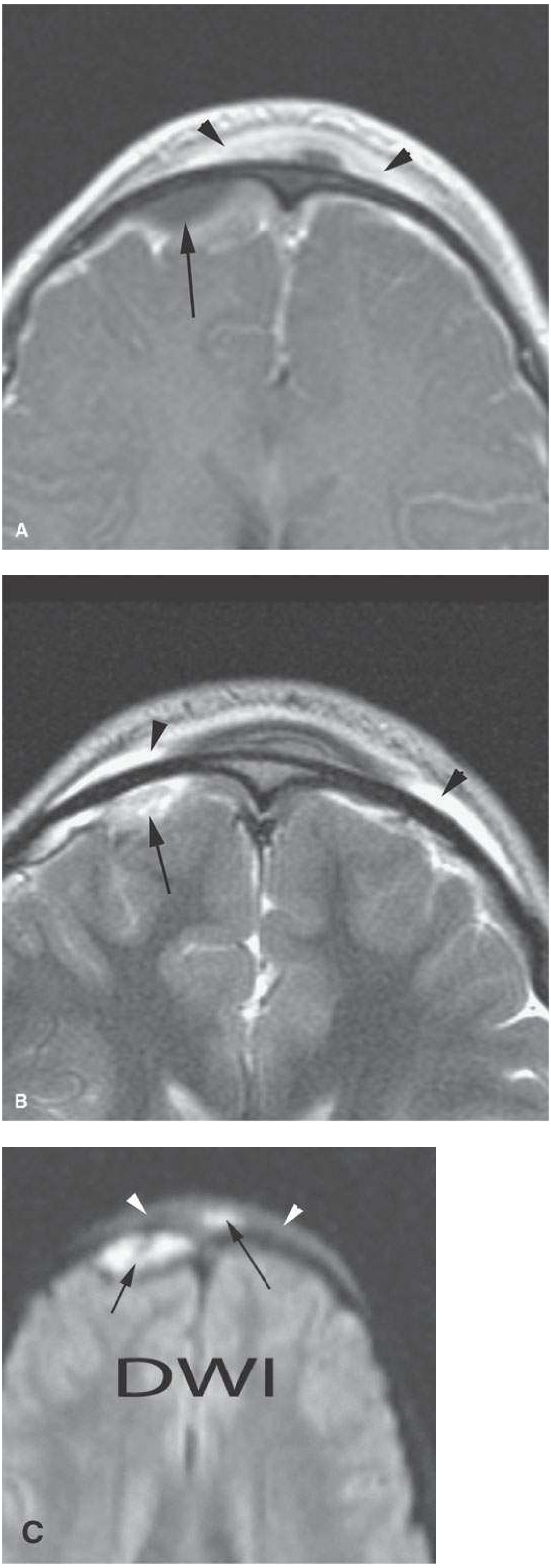
A
B
DWI
C

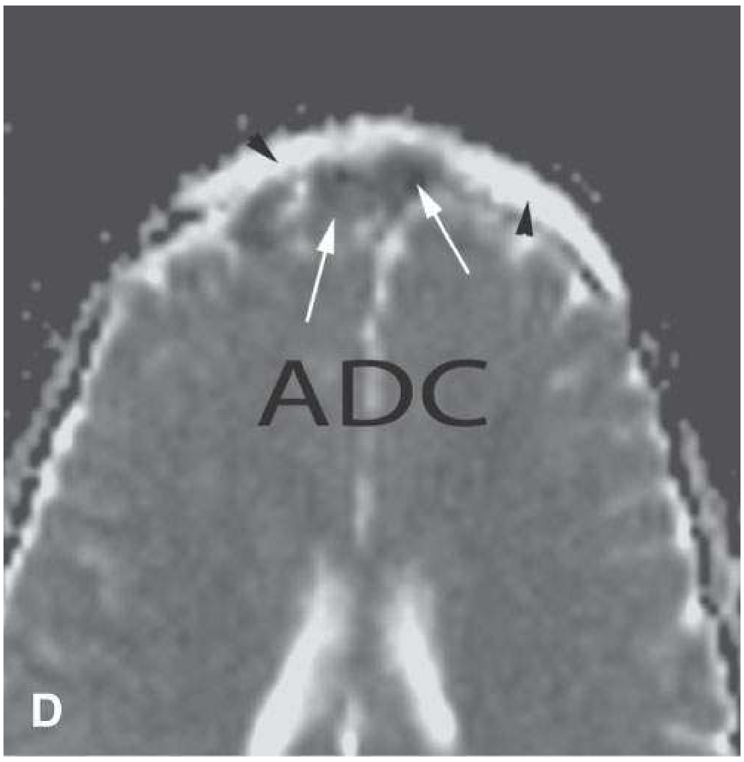


**FIGURE 10.29.** Magnetic resonance imaging of a patient with an epidural empyema and deep scalp abscess. **A:** T1-weighted contrast-enhanced image shows the epidural empyema *(arrow)* and scalp edema *(arrowheads)* with a small, likely subgaleal, abscess. **B:** T2-weighted image shows the two abscesses as in **(A)** *(arrow)* and related scalp edema *(arrowheads)*. Diffusion-weighted image **(C)** and apparent diffusion coefficient (ADC) map **(D)** show restricted diffusion in the abscesses *(arrows)* but not in the scalp edema *(arrowheads)*.

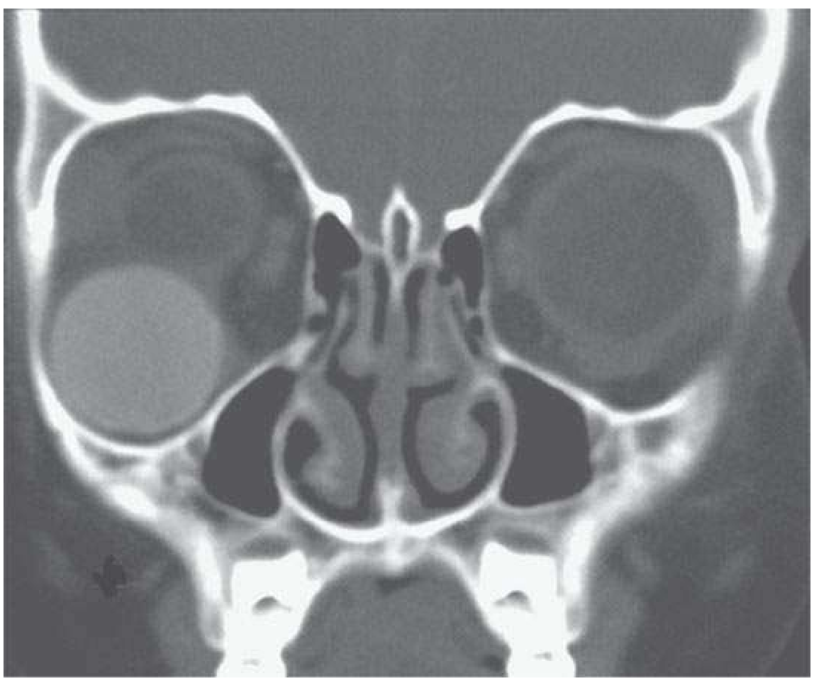

**FIGURE 10.30.** Computed tomography (CT) of a dermoid cyst of the orbit that is high density compared to muscle—a fairly atypical finding even in these developmental cysts as they are seen on CT.

An almost unique appearance can sometimes lead to a very specific diagnosis that otherwise may not have been considered. A common example of this is the low neck cystic lymph node with and avid enhancing mural nodule that is very characteristic of a nodal metastasis due to papillary thyroid cancer sometimes seen in the absence of a visible nodule in the gland (Fig. 10.31).[1,6]

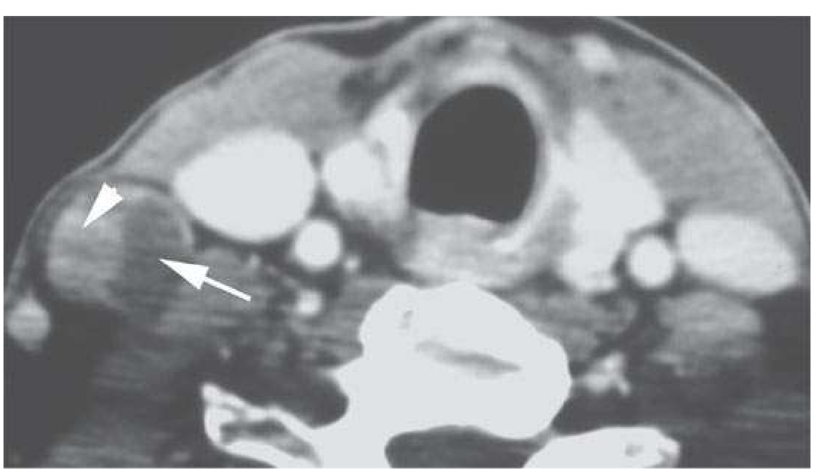

**FIGURE 10.31.** Contrast-enhanced computed tomography of a patient with a right level 4 neck mass. The cystic mass *(arrow)* with an enhancing nodule *(arrowhead)* in its wall is almost characteristic of thyroid cancer metastasis. A calcification would make that prime suspicion even more likely.

The thicker or more enhancing the capsule or pseudocapsule of a cystic mass, the more likely the collection is infected (Figs. 10.5, 10.22, 10.23, and 10.32) or is a tumoral cyst (Figs. 10.31 and 10.33), but this is by no means specific. Extensive surrounding soft tissue swelling consistent with edema and/or cellulitis also supports the suspicion of infection but is not diagnostic of that condition (Figs. 10.5, 5.10, and 22.10). Less perifocal edema suggests a tumoral cystic collection or partially treated and/or chronic infectious process (Figs. 10.9 and 10.11)

**FIGURE 10.23.** Contrast-enhanced computed tomography of a patient with an acute, untreated subperiosteal abscess of the floor of the mouth with a typical shape of pus spreading between the bone and periosteum. It shows a thick, enhancing margin *(black arrow)*, low-density fluid collection, and surrounding cellulitis and edema manifest by thickening of the superficial musculoaponeurotic system (SMAS) layer *(arrowhead)* and subcutaneous edema *(white arrow)*.

**FIGURE 10.32.** Contrast-enhanced computed tomography of a patient with a dentigerous cyst of the mandible that became secondarily infected. The infected collection *(black arrow)* is surrounded by a fairly typical confirmatory inflammatory response *(white arrow)*.

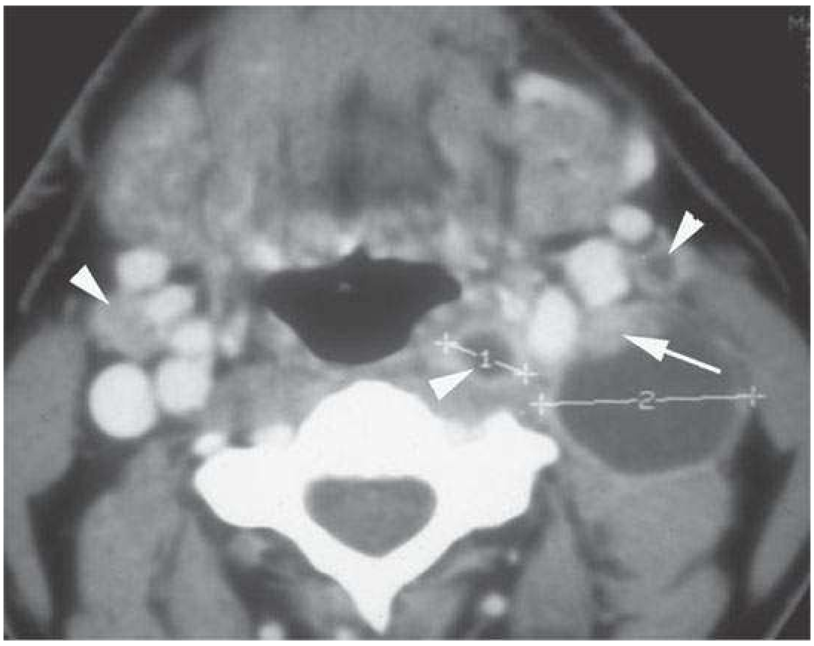

**FIGURE 10.33.** Contrast-enhanced computed tomography of a relatively thin walled level 2 mass. The mural nodules and other metastatic nodes *(arrowheads)* become a clue to the etiology. In contrast to inflammatory collections, there is little if any reactive change or edema around the largest of the metastatic nodes.

Calcification may be dystrophic (Chapter 12) or be a clue to a cystic neoplasm.

Septations are generally not useful in differential diagnosis except to classify the cyst as complex (Fig. 10.25). A multiseptated appearance can be useful in identifying lesions such as the various venolymphatic malformations (Chapter 9), given the correct clinical context.

Fluid–fluid levels may result from acute or chronic bleeds and the resulting evolution of the blood products (Fig. 10.2), and those blood products themselves may also help in identifying common problems such as cholesterol granulomas (also referred to as cholesterolosis) (Fig. 10.34), bleeds into venolymphatic malformations, and the rare aneurysmal bone cysts. In a rapidly enlarging mass, a fluid–fluid level can help suggest bleeding as an etiology for the rapid enlargement (Fig. 10.2).

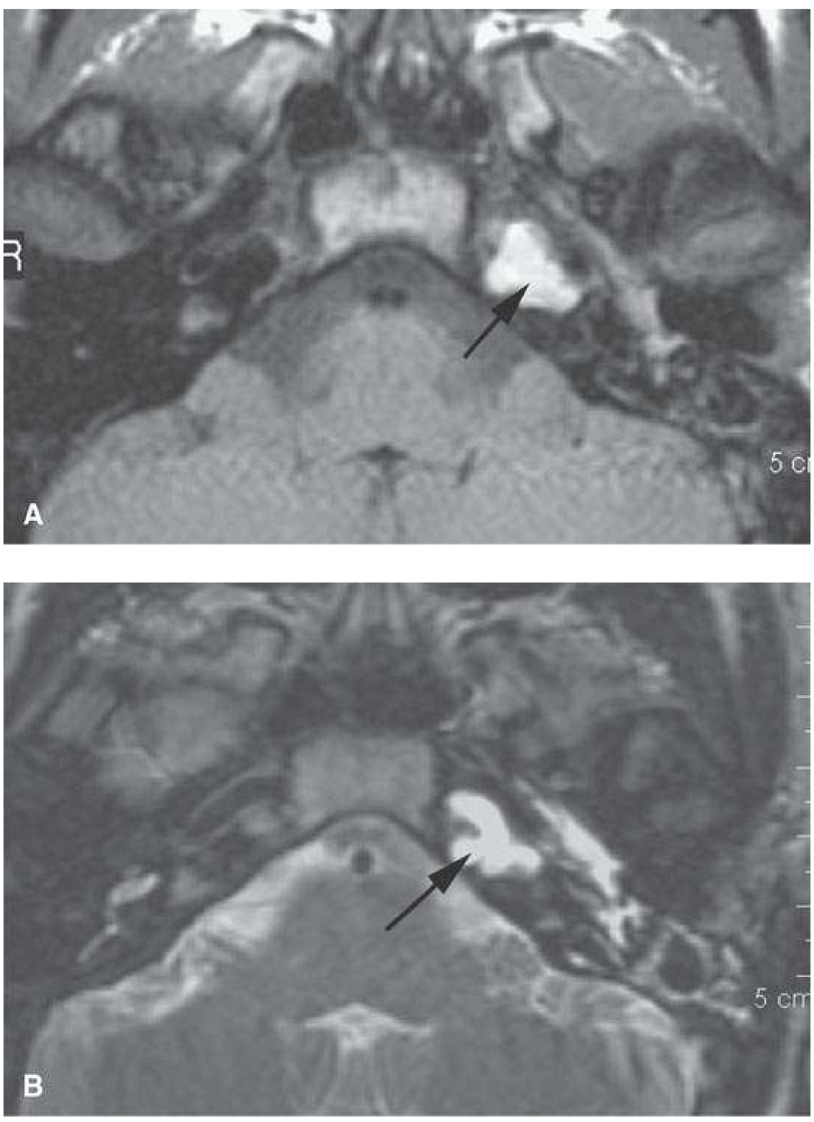


**FIGURE 10.34.** Magnetic resonance imaging of a patient with surgically proven cholesterolosis (cholesterol granuloma) of the petrous apex. **A:** TI-weighted non–contrast-enhanced image shows the bright signal *(arrow)* petrous apex due to cholesterol in solution and/or chronic blood products. **B:** T2-weighted image is nonspecific, showing only that this is likely some sort of fluid collection *(arrow)* or possibly an epidermoid cyst since low signal of chronic blood products could not be confirmed.

The presence of gas and/or and air fluid level suggests infection or connection to the skin or gastrointestinal tract (Fig. 10.35) or iatrogenic introduction of gas by a prior puncture or attempted drainage procedure (Fig. 10.36).

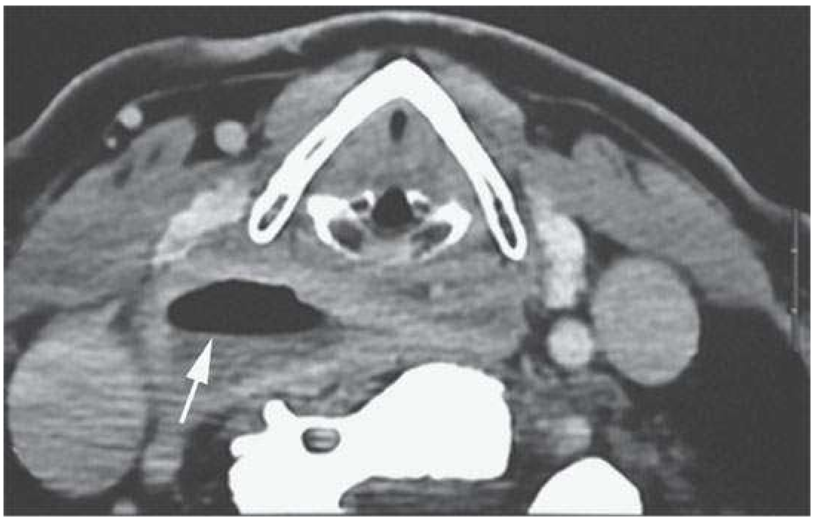

**FIGURE 10.35.** Contrast-enhanced computed tomography image shows an air–fluid level in the retropharyngeal space and deep neck *(arrow)* due to connection with the gastrointestinal tract and identifying it as a Zenker diverticulum.

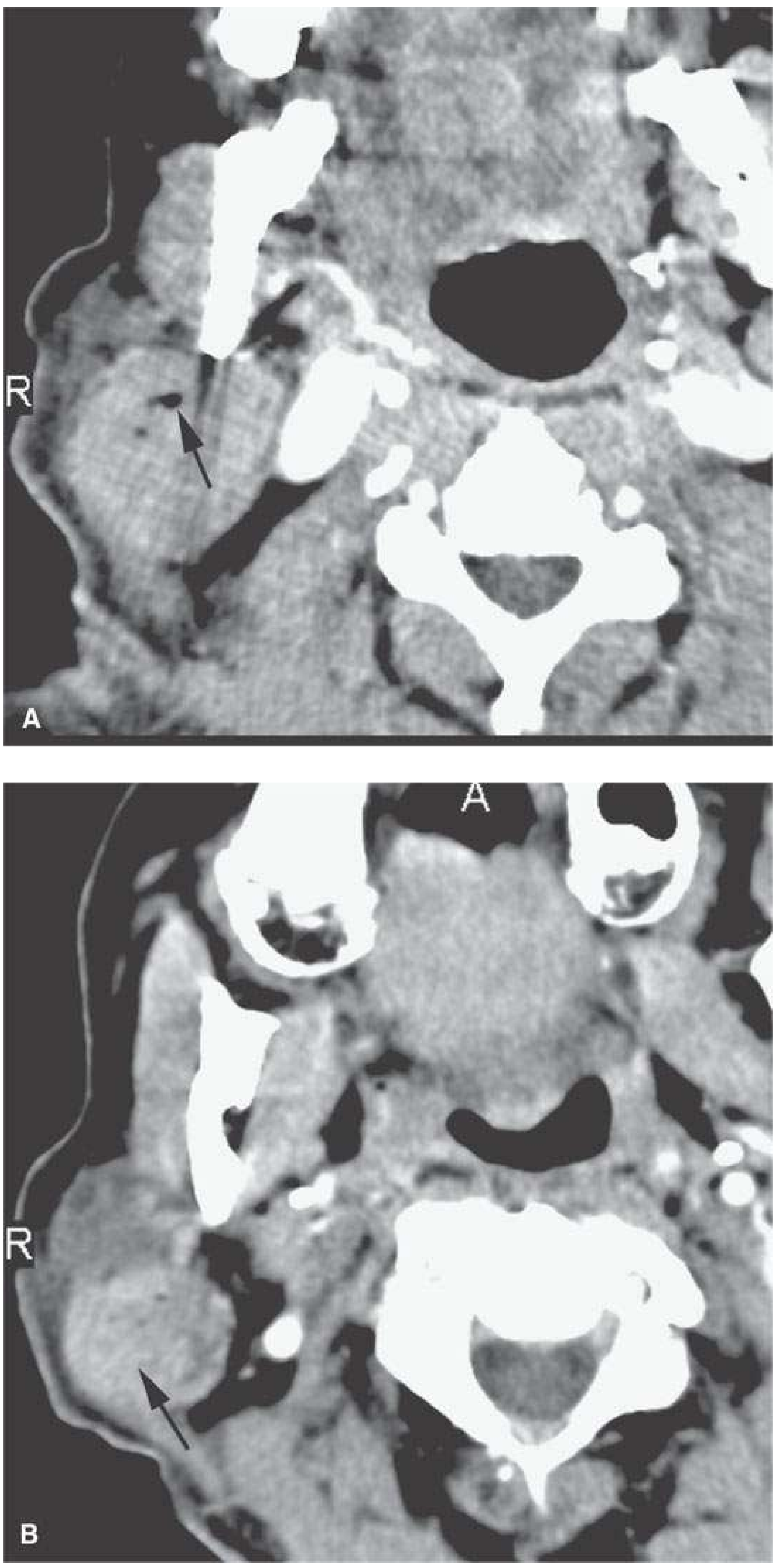


**FIGURE 10.36.** Non–contrast-enhanced computed tomography **(A, B)** showing gas *(arrow)* in a fluid collection that is of higher density than muscle. The gas is due to the needle stick; the high-density fluid collection is due to the acute hematoma.

# MAGNETIC RESONANCE AND COMPUTED TOMOGRAPHY APPEARANCE

On CT, the apparent density of fluid collections will vary from obviously water or cerebrospinal fluid (CSF)-like or equivalent to and sometimes beyond that of skeletal muscle or greater (Figs. 10.5 and 10.36).[5,8,9] Fluid collections that are hyperdense with respect to muscle are less common than those that are hypodense to muscle on CT. The hyperdense appearance suggests blood products, cholesterol in solution (Fig. 10.30), desiccation (Fig. 10.26), or calcification. Hyperdense collections are most common in the sinuses.

As with brain lesions, the small septations of a microcystic mass will normally not be resolved on CT; thus, both micro- and macrocystic areas may appear homogeneous. This is perhaps most commonly observed in cystic-appearing, usually benign salivary gland neoplasms. MRI does a much better job at identifying this likely pathoanatomic pattern than does CT or ultrasound (US) (Fig. 10.37).

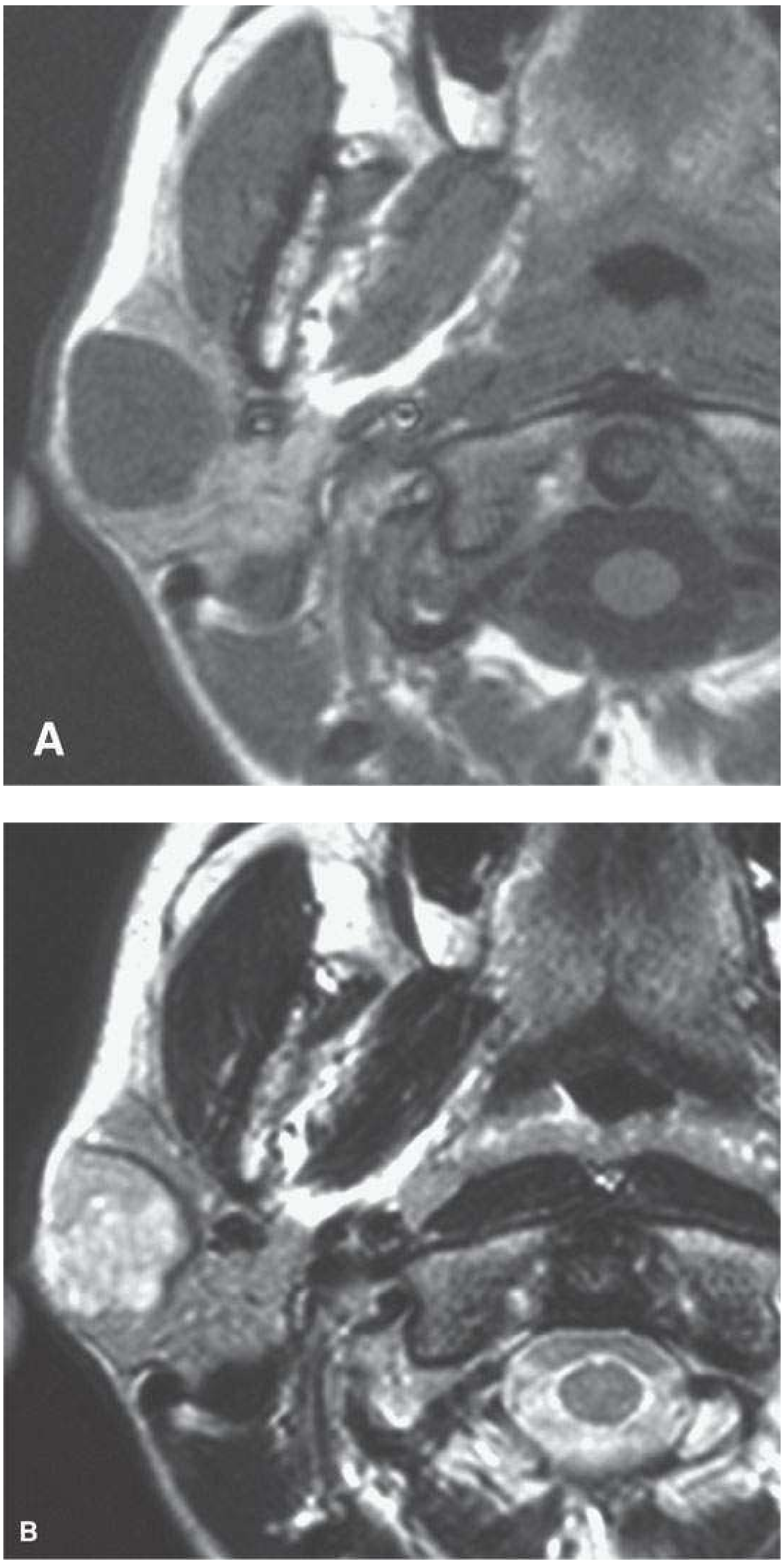

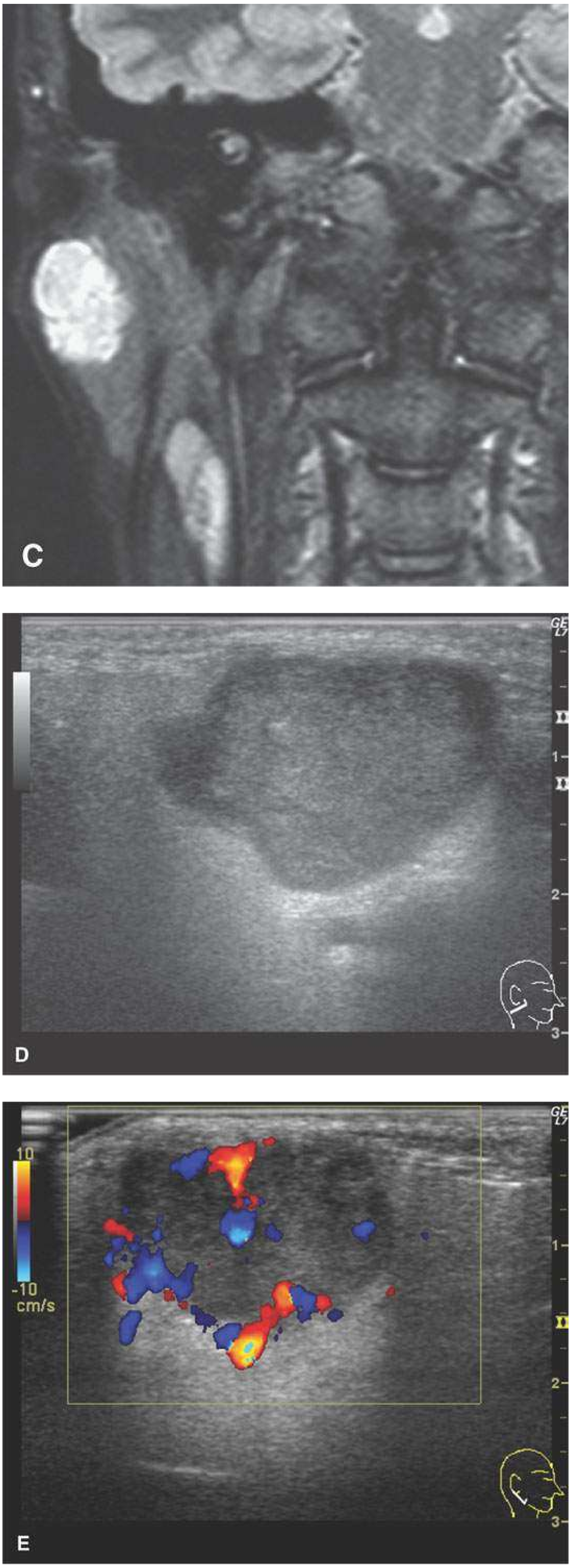


**FIGURE 10.37.** Magnetic resonance imaging and ultrasound of a patient with a benign mixed tumor. The behavior as seen on a T1-weighted non–contrast-enhanced image **(A)**, T2-weighted image **(B)**, and short T1 inversion recovery (STIR) image **(C)** are consistent with the microcystic structure of this benign neoplasm. The B-mode ultrasound image **(D)** also reflects the microcystic morphology, but the color flow image shows obviously internal vascularity consistent with the diagnosis of a neoplasm.

Contrast-enhanced computed tomography (CECT) will normally show the wall of the cyst or border of a fluid collection with greater clarity than a non–contrast-enhanced computed tomography (NCCT) study (Figs. 10.19 and 10.20).9,10 This is true even in noninfected cysts, either due to enhancement of surrounding structures or due to "low-grade" enhancement in a reactive but not infected capsule or pseudocapsule (Figs. 10.17 and 10.18).

On MRI, the appearance of fluid collections varies greatly with the pulse sequence and intravenous contrast enhancement.8–10 On T1W spin echo (SE) sequences, the intensity of a fluid collection may vary anywhere from isointense to CSF to an intensity between muscle and fat (Figs. 10.4A, 10.6A, 10.12A, 10.19A, and 10.26C). Intensities frequently are in the range between muscle and fat in the absence of hemorrhage, especially in the paranasal sinuses (Fig. 10.26). On T2W SE images, fluid areas are often as bright as or brighter than CSF because the fluid is static, but there is a wide range of signal intensities possible (Fig. 10.27B). The behavior of fluid collections on gradient echo and inversion recovery, including short T1 inversion recovery (STIR) images, and fat-suppressed images will depend on the relative T1, T2, and proton density weighting of the sequences (Figs. 10.2 and 10.37C).

Contrast-enhanced magnetic resonance (MR), like CECT, tends to show the margins of a fluid collection with more clarity on T1W images than a non–contrast-enhanced MR study, and the degree to which this is true depends in large part on the etiology of the cyst and the nature of its capsule or pseudocapsule (Figs. 10.4C and 10.19B). If the cyst is bordered by fat, fat-suppressed postcontrast T1W images will define the cyst wall in a manner equivalent to or better than CT (Fig. 10.4C).

The water and protein content of the cyst are the most important factors creating the CT and MR appearance just described. On CT, desiccation and increased protein content raise electron density that produces a concomitant rise in CT density (Chapters 1 and 3). The effects of drying are best illustrated by the progressive increase in density of clinically inspissated sinus secretions (Figs. 10.26 and 10.38). On rare occasions, fat, such as seen in a chylous effusion, will make a fluid collection more lucent. Calcium in solution may cause CT fluid collections to appear extraordinarily dense.

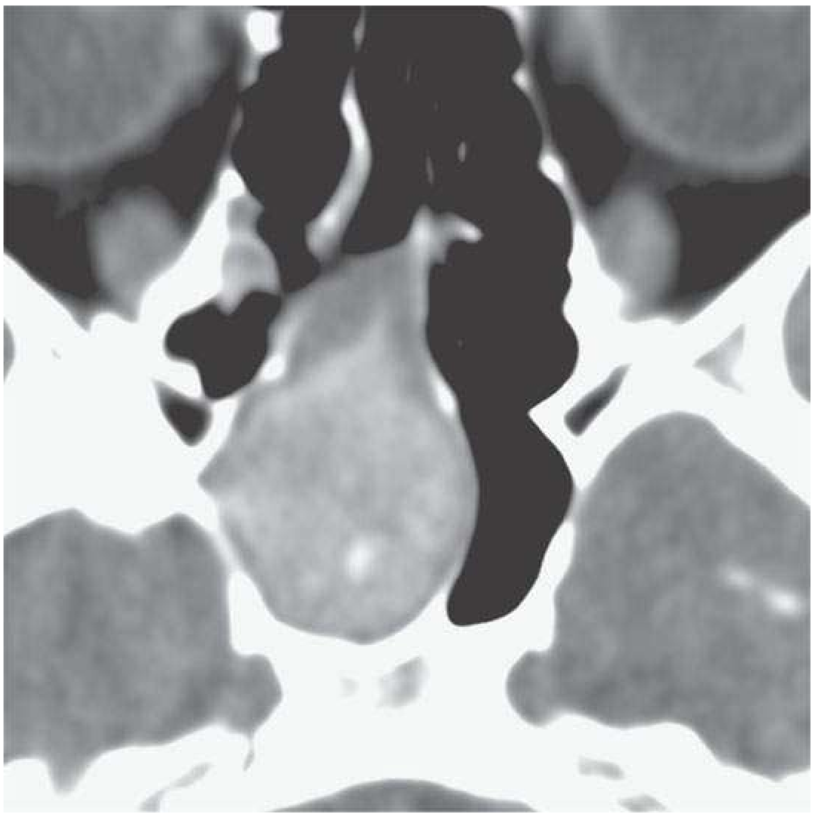

**FIGURE 10.38.** Non–contrast-enhanced computed tomography (CT) showing that progressive desiccation of sinus secretions can commonly lead to a CT density far greater than fluid and muscle to the point sometimes of simulating calcification.

With MR, the effects of protein and water are more complex than with CT because the physical state of water and protein affect proton relaxation (Chapters 1 and 3). In general, diminished free water content shortens T1 and T2 (Fig. 10.4A,B). The presence of protein in water increases both the effects of local static magnetic fields (T2 shortening effect) and the number of molecules tumbling within the resonant range surrounding the Larmor frequency (T1 shortening effect) (Figs. 10.6B and 10.26B). The rationale for these effects is discussed in conjunction with the physical properties that give rise to MRI signal intensity seen on various pulse sequences (Chapter 3).

Other substances within fluid collections or cysts will affect the MR signal. Cholesterol, in solution, produces profound T1 shortening while having very little visual impact on T2W images since cholesterol tumbles near the Larmor frequencies, but its presence has less relative effect on local static magnetic fields (Fig. 10.34 and Chapter 3). A good extracranial example of this is the Tornwaldt cyst (Fig. 10.6) that behaves similar to intracranial fluid-containing structures such as the Rathke cleft cyst and colloid cyst of the third ventricle, all of which frequently have increase in signal intensity on T1 and T2W images.8–10 Similar effects of cholesterol in solution are also seen in some dermoid cysts and areas of chronic hemorrhage such as cholesterolosis of the petrous apex and posttraumatic hematocyst (Fig. 10.34). In the latter two lesions, the cholesterol is the end stage of unresorbed blood breakdown products.

Epidermoid cysts contain flaky or waxy keratin debris that is very rich in cholesterol crystals; however, in the cerebellopontine angle, these lesions are typically of low signal intensity on T1W images (Chapter 8).8,9,10 In a typical intracranial epidermoid cyst, cholesterol simply is not in a physical state that will allow as many of the hydrogen molecules to tumble, at a rate equivalent to the operating Larmor frequency, so there is no obvious T1 shortening. The structure of the interstices of this cyst is then better represented by the restricted diffusion noted on DWI (Chapter 8). Some “epidermoid” cysts, however, show profound T1 shortening (without apparent hemorrhage pathologically), thus suggesting that the cholesterol must be partly in solution (Chapter 8). There are reports of epidermoid cysts appearing hyperdense to brain on CT. The physical state of the water content can be further evaluated with DWI. In the more highly structured lesions such as an epidermoid cyst and with mucopurulent collections, diffusion will be restricted (Figs. 10.27–10.29).

Blood products cause confusion during MR interpretation. On CT, visualization of blood products is simply related to the protein content and structure of the clot/hematoma (Fig. 10.20A) rather than the oxidation of the iron and evolution of the globin and other protein content of a clot. On MR, the relative protein and water content and paramagnetic properties of degraded hemoglobin combine to produce profound changes at the site of hemorrhage. The appearance is linked to the rate of clot lysis with breakdown of the red cells and degradation of the hemoglobin molecule. These factors are further influenced by location and whether there have been repeated episodes of hemorrhage (Fig. 10.39). Since the area of bleeding is usually sampled at one point in its evolution, a rigid approach that involves assigning specific time frames to certain MR findings may lead to confusion. It is essential to recognize that the findings are related to hemorrhage in order to construct an accurate diagnosis. A basic timetable based on the physical principles of MR as well as clot evolution that is discussed in detail elsewhere is a useful outline for evaluating the approximate age of hemorrhage and variable appearance of blood products as see on MR images (Chapters 1, 3, and 10).

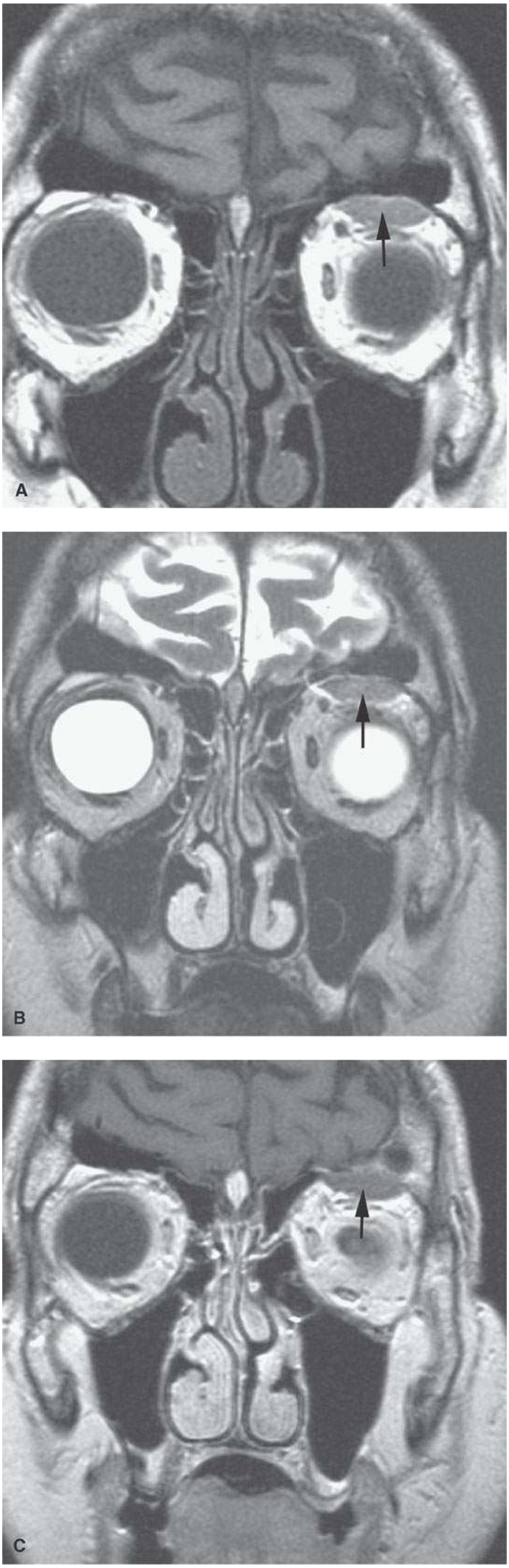
A
B
C

**FIGURE 10.39.** Magnetic resonance imaging of a patient with a subacute orbital subperiosteal hematoma induced by straining. **A:** T1-weighted non–contrast-enhanced image shows the collection of blood *(arrow)* to be isointense to brain. **B:** T2-weighted image shows that the collection *(arrow)* is still relatively isointense to brain. **C:** There is no change on the T1-weighted contrast-enhanced image *(arrow)*. The combination of findings is consistent with an organized, subacute clot not yet having undergone significant clot lysis or conversion of hemoglobin to methemoglobin.

# ULTRASOUND APPEARANCE

Fluid collections on US are generally described as simple or complex.[11] Complex cysts are those with thick or irregular or frankly nodular walls, septations, fluid–fluid levels, and/or debris within the fluid (Figs. 10.4D,E; 10.10; and 10.13) Microcystic masses such as those in the salivary glands can mimic more purely macrocystic lesions and vice versa (Figs. 10.10 and 10.37D,E).

Many other features potentially useful in differential diagnosis that are easily seen on CT and/or MRI may not be apparent on US. Associated pathology and the full extent of the collection may be difficult to determine with US; thus, in most instances, when a lesion can be reached by the transducer, outside of the thyroid gland, the added information from US is not definitive and is cost additive, producing little additional benefit (Figs. 10.10 and 10.13). The exception to this is in the thyroid, where identification of a thyroid nodule as purely or >75% cystic is a very useful triage parameter for assessing cancer risk in a nodule (Figs. 10.4 and 10.15).

Color flow Doppler US can add important flow-related information that can help avoid a potential disastrous misinterpretation of a solid lesion as cystic or aggressive needle sampling of a lesion of blood vessel origin (Figs. 10.4, 4.10, and 15.10).

## *Suggested Readings*

Gritzmann N, Hollerweger A, Macheiner P, et al. Sonography of soft tissue masses of the neck. *J Clin Ultrasound*. 2002;30(6):356–373.

Koch BL. Cystic malformations of the neck in children. *Pediatr Radiol*. 2005;35(5):463–477.

Thompson LD. Diagnostically challenging lesions in head and neck pathology. *Eur Arch Otorhinolaryngol*. 1997;254(8):357–366.

Turkington JR, Paterson A, Sweeney LE, et al. Neck masses in children. *Br J Radiol*. 2005;78(925):75–85.

Wippold FJ II. Head and neck imaging: The role of CT and MRI. *J Magn Reson Imaging*. 2007;25(3):453–465.

## *References*

1. Shefelbine SE, Mancuso AA, Gajewski BJ, et al. Pediatric retropharyngeal lymphadenitis: Differentiation from retropharyngeal abscess and treatment implications. *Otolaryngol Head Neck Surg*. 2007;136(2):182–188.

2. Gupta RK, Naran S, Lallu S, et al. The diagnostic value of fine needle aspiration cytology (FNAC) in the assessment of palpable supraclavicular lymph nodes: A study of 218 cases. *Cytopathology*. 2003;14(4):201–207.

3. Saboorian MH, Ashfaq R. The use of fine needle aspiration biopsy in the evaluation of lymphadenopathy. *Semin Diagn Pathol*. 2001;18(2):110–123.

4. Yuca K, Etlik O, Kiroglu AF, et al. Endoscopic view and MRI of a Thornwaldt's cyst of the nasopharynx. *B-ENT*. 2005;1(3):155–157.

5. Koch BL. Cystic malformations of the neck in children. *Pediatr Radiol*. 2005;35(5):463–477.

6. Ahuja A, Ng CF, King W, et al. Solitary cystic nodal metastasis from occult papillary carcinoma of the thyroid mimicking a branchial cyst: A potential pitfall. *Clin Radiol*. 1998;53(1):61–63.

7. Benson MT, Dalen K, Mancuso AA, et al. Congenital anomalies of the branchial apparatus: Embryology and pathologic anatomy. *Radiographics*. 1992;12(5):943–960.

8. Setoguchi T, Hasuo K, Shida Y, et al. Second branchial cleft cyst with "cyst-within-cyst" appearance. *Clin Imaging*. 2007;31(5):352–355.

9. Khanna G, Sato Y, Smith RJ, et al. Causes of facial swelling in pediatric patients: Correlation of clinical and radiologic findings. *Radiographics*. 2006;26(1):157–171.

10. Vazquez E, Enriquez G, Castellote A, et al. US, CT, and MR imaging of neck lesions in children. *Radiographics*. 1995;15(1):105–122.

11. Ahuja A, Ying M. Sonographic evaluation of cervical lymphadenopathy: Is power Doppler sonography routinely indicated? *Ultrasound Med Biol*. 2003;29(3):353–359.